National Park Service
U.S. Department of the Interior

Natural Resource Stewardship and Science

Monitoring Vegetation Change in Coastal Marshes of Southwest Alaska, 2007–2018

Natural Resource Report NPS/SWAN/NRR—2020/2202

ON THIS PAGE
A coastal brown bear grazing on salt marsh vegetation at Silver Salmon Creek, LACL
Photo credit: NPS/MICHAEL HANNAM

ON THE COVER
Southwest Alaska Network scientists perform point-intercept vegetation sampling at a monitoring plot in Hallo Bay, KATM
Photo credit: NPS/MICHAEL HANNAM

Monitoring Vegetation Change in Coastal Marshes of Southwest Alaska, 2007–2018

Natural Resource Report NPS/SWAN/NRR—2020/2202

Michael P. Hannam, Amy E. Miller, and James K. Walton

Southwest Alaska Inventory & Monitoring Network
National Park Service
240 W 5th Avenue
Anchorage, AK 99501

December 2020

U.S. Department of the Interior
National Park Service
Natural Resource Stewardship and Science
Fort Collins, Colorado

The National Park Service, Natural Resource Stewardship and Science office in Fort Collins, Colorado, publishes a range of reports that address natural resource topics. These reports are of interest and applicability to a broad audience in the National Park Service and others in natural resource management, including scientists, conservation and environmental constituencies, and the public.

The Natural Resource Report Series is used to disseminate comprehensive information and analysis about natural resources and related topics concerning lands managed by the National Park Service. The series supports the advancement of science, informed decision-making, and the achievement of the National Park Service mission. The series also provides a forum for presenting more lengthy results that may not be accepted by publications with page limitations.

All manuscripts in the series receive the appropriate level of peer review to ensure that the information is scientifically credible, technically accurate, appropriately written for the intended audience, and designed and published in a professional manner.

This report received formal peer review by subject-matter experts who were not directly involved in the collection, analysis, or reporting of the data, and whose background and expertise put them on par technically and scientifically with the authors of the information.

Views, statements, findings, conclusions, recommendations, and data in this report do not necessarily reflect views and policies of the National Park Service, U.S. Department of the Interior. Mention of trade names or commercial products does not constitute endorsement or recommendation for use by the U.S. Government.

This report is available in digital format from Southwest Alaska Network and the Natural Resource Publications Management website. If you have difficulty accessing information in this publication, particularly if using assistive technology, please email irma@nps.gov.

Please cite this publication as:

Hannam, M. P., A. E. Miller, and J. K. Walton. 2020. Monitoring vegetation change in coastal marshes of Southwest Alaska, 2007–2018. Natural Resource Report NPS/SWAN/NRR—2020/2202. National Park Service, Fort Collins, Colorado. https://doi.org/10.36967/nrr-2280108.

NPS 953/173876, December 2020

Contents

Figures

Page

Figures (continued)

Page

Tables

Appendices

Executive Summary

Coastal marshes and meadows cover a small area in Southwest Alaska Network (SWAN) parks but are heavily used by wildlife, migratory birds, and park visitors. They are of particular value to brown bears, which frequent them for early season forage, and critical mating and rearing habitat for their young.

To understand how coastal marshes are changing through time, and to inform park planning and decision making in these valued habitats, the SWAN monitors vegetation composition at three sites at Katmai (KATM) and Lake Clark (LACL) national parks and preserves (Jorgenson & Miller 2010). In 2007 and 2008, we conducted baseline monitoring at these sites in LACL and KATM, respectively, and in 2018, we resurveyed the sites in our first 10-year revisit to measure change. We also added three new monitoring sites in Kenai Fjords National Park (KEFJ) in 2018.

Our results from the 2018 resurveys in LACL and KATM showed that, in general, plant communities have remained relatively stable between the 2007–2008 and 2018 sampling events. However, we also recorded localized and broad-scale changes across the sites. The habitat divisions and floristic classes identified in 2007–2008 by Jorgenson et al. (2010) still capture more than half of the variation in community composition among plots. However, we measured an increase in cover of vascular plants in 2018, and isolated cases of community-level change, indicated by a change in some floristic classes between 2007–2008 and 2018. The widespread increase in vascular plant cover that we observed between 2007–2008 and 2018 may have resulted from an earlier green-up in 2018, and/or from increases in productivity during the decade between the first and second sampling dates.

Although we cannot infer a trend from two points in time, the changes recorded from our field measurements between 2007–2008 and 2018 are largely consistent with the longer-term ecosystem changes reported by Jorgenson et al. (2010) in their comparison of images from the 1950s, 1980s and early-mid 2000s. These changes, interpreted from imagery (Jorgenson et al. 2010), included vegetation establishment on barren substrates (e.g., beach berms), drying and infilling of ponds, and expansion of spruce cover on outer beach ridges. Our field data from 2018 likewise showed rapid colonization of beach dunes and mudflats, increases in spruce cover, and expansion of shrubs at upper meadow margins. Our results suggest that coastal marshes have not undergone site-wide changes in the last decade but may be showing changes in localized areas, consistent with changes reported over the last half-century by Jorgenson et al. (2010).

Acknowledgments

Staff at AKRO, KEFJ, KATM, LACL, and SWAN were instrumental in supporting our field data collection. We would like to offer specific thanks to Kara Lewandowski (LACL) and Christina Kriedeman for their local knowledge and on-the-ground support. In the air, Don Welty (LACL), Rich Richotte (LACL), Troy Hamon (KATM), Adam Grenda (KATM), Paul Anderson (AKRO) and Jeff Babcock (AKRO) flew us safely to our coastal field sites. On the R/V Serac, Brandon Russel and Nathanial Charbonneau (KEFJ) provided excellent support for our KEFJ fieldwork. Emily Platt (SWAN) and Christina Kriedeman (KEFJ) shared long hours in the field with us collecting vegetation data, and managed smiles through all kinds of conditions. Sarah Brey (SWAN) assisted with data analysis for the report. Tim Shepherd and Russ Frith (SWAN) created our field database and wrangled data from the baseline monitoring to facilitate our analyses. We would have been lost without the support of Joel Cusick (AKRO) who always had us equipped with the GPS equipment that we needed. Thank you to Celia Miller and David Swanson (ARCN) for providing detailed, thoughtful reviews that greatly improved this report, and Jim Lawler orchestrating the review. Thanks to Carlene Miller (SWAN) for her detailed formatting of this report.

Introduction

Coastal marsh monitoring in the Southwest Alaska Network (SWAN) focuses on habitat characteristics that support other nearshore and terrestrial indicators (e.g., brown bears, seabirds, and bivalves). Monitoring sites are located in salt marshes on the coasts of Katmai (KATM) and Lake Clark (LACL) National Parks and Preserves, and brackish coastal meadows of Kenai Fjords (KEFJ) National Park (Figure 1). Salt marsh and coastal meadow habitats comprise a small proportion of the area in SWAN parks, yet are heavily used by wildlife, migratory birds, and park visitors. They provide valuable ecosystem services, among them early season forage and critical mating and rearing habitat for brown bears in sedge-dominated (e.g., *Carex ramenskii*) meadows (Bennet 1996), and foraging habitat for migratory shorebirds (Bennet 1996; Gill, Jr. & Tibbitts 1999). These marshes are dynamic systems and are subject to perturbation by a range of factors, including warming temperatures, storm surges, tectonic uplift, and development-related activities.

Salt marshes in Upper Cook Inlet and along Shelikof Strait occur as low-lying, saline areas comprising active tidal flats subject to frequent tidal inundation, and inactive tidal flats characterized by brackish to slightly brackish soils (Jorgenson et al. 2003). Well-drained beach ridges and levees support beach rye (*Leymus mollis = Elymus arenarius* subsp. *mollis*) meadows, alder (*Alnus viridis* subsp. *sinuata*) strands, and Sitka/Lutz spruce (*Picea sitchensis/P. x lutzii*), while loamy, often poorly-drained basins support halophytic vegetation and/or sweetgale (*Myrica gale*)-graminoid shrub meadows (Jorgenson et al. 2003, 2010). Near KEFJ, in western Prince William Sound, salt marshes are rare, but beach rye is a widespread species on dunes, flood plains, beaches, and in estuaries (DeVelice et al. 1999).

Change in salt marshes can result from many drivers. Salt marshes exist in a dynamic balance among forces of sedimentation, erosion, subsidence, relative sea level change, and vegetation growth (Redfield 1965, 1972; Morris et al. 2002). Changes to any of these processes may affect the trajectory of the marsh. Barrier beaches can be reshaped by coastal processes and may be breached by storm surges or tidal channel migration, altering tidal inlets to the marsh and sediment dynamics. Sediment supply from nearby river systems may change due to glacial advance or retreat or from ash and lahar deposits. Relative sea level may rise or fall depending on the balance of global sea level rise, regional tectonic movement, and isostatic rebound. Within a marsh, tidal channels may migrate, disturbing existing vegetation and creating new substrate for colonization. Increasing temperature is expected to change the rates of biological processes, and is likely to result in increased primary productivity in the meadows (Kirwan & Blum 2011).

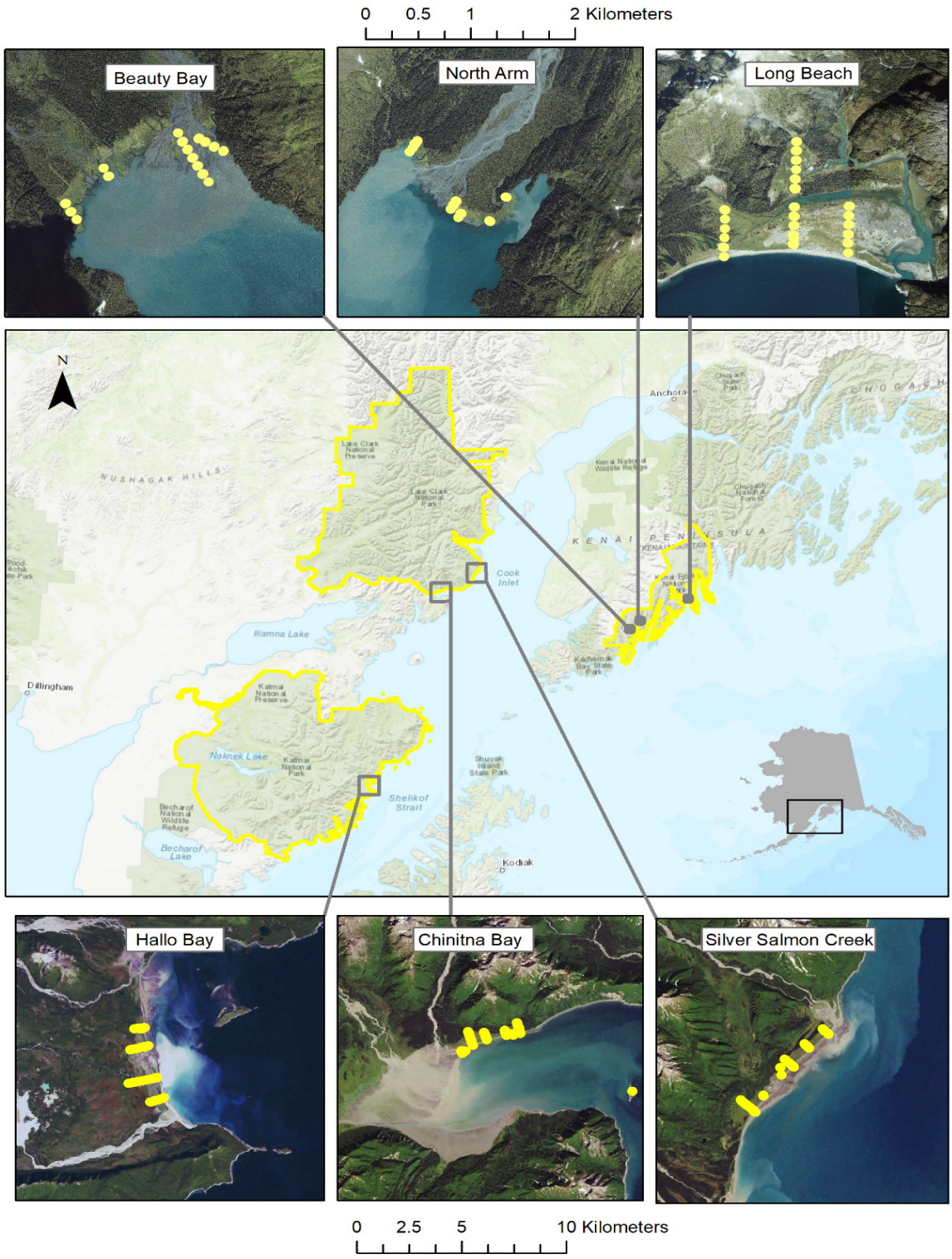

Figure 1. Salt marsh monitoring sites in Kenai Fjords National Park (top), Katmai National Park & Preserve (bottom left), and Lake Clark National Park & Preserve (bottom center and right). Chinitna Bay (CHBA) and Silver Salmon Creek (SISA) were initially sampled in 2007. Hallo Bay (HABA) was first sampled in 2008.

Worldwide, many salt marshes are threatened by accelerating sea level rise and coastal development (Kennish 2002; Kirwan & Megonigal 2013), but in coastal southwest Alaska, tectonic activity and isostatic rebound have led to complex, locally variable relative sea level change (Shugar et al. 2014). Models extrapolating from global positioning system (GPS) time series indicate that the northwest coast of Cook Inlet has experienced declining relative sea-level (Freymueller et al. 2013). Uplift following the magnitude 9.2 earthquake of 1964 has resulted in the conversion of former mudflats to coastal meadows in Chinitna Bay (Jorgenson et al. 2006), and the establishment of spruce in what were formerly wet meadows (Jorgenson et al. 2010). A comparison of aerial photos and satellite imagery from Silver Salmon Creek (LACL), Chinitna Bay (LACL) and Hallo Bay (KATM) in the 1950s and early-mid 2000s have shown a roughly 6% increase in coastal gravelly saline barrens, due to uplift and shoreline accretion that extended beaches seaward; and a 1%–2% decrease in coastal brackish ponds, due to drainage and/or accumulation of organic matter (Jorgenson et al. 2010).

More localized physical forces also affect these marshes through accretion and erosion. Storm surges, a major driver of coastal vegetation change in western Alaska (Jorgenson et al. 2018), have resulted in shoreline migration, reconfiguration of surficial deposits at river mouths, overwash deposits across the beach ridges, and sedimentation on tidal flats at all three sites in LACL and KATM (Jorgenson et al. 2010). The result of these changes has been the loss of vegetation in some locations due to erosion and/or frequent flooding, and the accretion of new substrate in others. In contrast, an analysis of repeat photos from our sites in LACL and KATM have shown that the larger tidal guts have remained stable over the past 50 years (Jorgenson et al. 2010). In sum, these forces of accretion and erosion have maintained a mosaic of early and later successional plant communities and unvegetated areas throughout the marshes, particularly on beach ridges and in low-lying, frequently inundated areas.

Based on our knowledge of these drivers of vegetation change and the changes documented in Jorgenson & Miller (2010), we expected to find evidence of continued drying in these meadows in 2018, and potentially an expansion of one or more of the dominant grass species, such as beach rye (*Leymus mollis = Elymus arenarius* subsp. *mollis*), circumpolar reedgrass (*Calamagrostis deschampsioides*), or bluejoint (*Calamagrostis canadensis*). We also expected to see an increase in spruce cover on beach ridges and in upper meadows, due to increases in stature in existing trees and possibly to new colonization by spruce seedlings. Finally, we expected that the reconfiguration of shorelines and channel banks would have generated new areas for early successional and/or salt-tolerant species to colonize.

This report summarizes coastal marsh vegetation monitoring to date in LACL and KATM (2007–2018), and vegetation plot establishment and initial sampling in KEFJ (2018). These revisits address two SWAN monitoring objectives laid out by Jorgenson & Miller (2010): (1) detect change in the cover and/or frequency of vascular plant species in the marsh and meadow communities through ground-based measurements; and (2) determine changes in the abundance and distribution of plant community types (floristic classes) across the gradient from upper marsh to shoreline.

Methods

Field Data Collection

Long-term vegetation monitoring plots were established in 2007 at Silver Salmon Creek and Chinitna Bay (LACL), and in 2008 at Hallo Bay (KATM; Figure 1). At each site, 4m × 10m plots were placed systematically at 100m intervals along four parallel transects that extended from the forest line at the upper marsh (upland, 0m) to the coastal shoreline. As Hallo Bay did not have a distinct forest-marsh transition, transects began in transitional birch/alder habitats. In addition to the systematically-located plots, subjectively-located plots were established in vegetation types that were under-represented in the systematic sample. Details of plot establishment are found in Jorgenson & Miller (2010).

Monitoring site revisits in 2018 consisted of re-measuring vegetation plots that had been established in 2007 and 2008. Species cover was estimated by point-intercept, as outlined in Jorgenson and Miller (2010) and Miller et al. (2010). In 2007 and 2008, vegetation point intercepts (hits) were recorded from the top of the canopy to the ground level, allowing for multiple hits per species per point, without separating out height classes. In 2018, hits were recorded in 4 different height classes (<0.5m, 0.5–1m, 1–4m, >4m above the ground) per point, allowing only a single hit per species per height class (Miller et al. 2010). For our analysis, we collapsed the hits from both visits to species presence-absence per point. In 2007 and 2008, point intercept data were collected using a rod-mounted laser pointer on a bubble-leveled handheld staff, in which the downward-pointing laser beam intercepted vegetation layers (Jorgenson & Miller 2010). In 2018, point-intercept cover data were collected using a similar handheld point-intercept staff, in which a fine-point rod (pin) was lowered to intercept vegetation (Miller et al. 2010).

In 2018, the within-plot sampling intensity was reduced from 100 points to 50 points at all but one monitoring plot, based on a power analysis conducted on the 2007–2008 data (Appendix A). Except where noted, taxonomic names in this report generally follow Jorgenson et al. (2010), for ease of comparison with their 2007–2008 results. Updated nomenclature and species codes are included in Appendix B.

Plot remeasurements in 2018 were scheduled to coincide closely with the day of year that they were sampled in 2007 and 2008. Part way through the 2018 field season, we realized that we were remeasuring the 4m × 10m plots on the opposite (e.g., south, or right) side of the upland-to-shoreline transects, relative to where they had been measured in 2007 and 2008 (e.g., north, or left side, looking down the transect from 0m). Plots measured in 2018 at Hallo Bay adjoin, but do not replicate plots measured in 2008. Hallo Bay was surveyed in mid-July, and plots were sampled on the opposite (south) side of the transect. Silver Salmon Creek was surveyed in July on the south side of the transect and re-measured on the correct (north) side in early September. Plots at Chinitna Bay were measured on the correct (north) side of the transect in August, one month later than the original survey date in 2007. To account for these spatial mismatches in data between the 2007–2008 and 2018 sampling events, we appended the cardinal direction from the transect end to the distant end of each 4m × 10m plot to the plot identifier (e.g., CHBA-T1-300-E). Plots were then grouped by their plot-block so that plots on the east and west side of the same transect point would be in a block for

subsequent analyses. For example, CHBA-T1-300-E and CHBA-T1-300-W would both fall in plot-block CHBA-T1-300.

As a part of the initial plot establishment in 2007 and 2008, each plot was assigned one of two geomorphic classes, Beach Ridge or Tidal Flat (Figure 2), and one of 17 floristic classes (List 1; Jorgenson et al. 2010). Floristic class assignment was based on a Two-way Indicator Species Analysis completed after the first sampling event (Jorgenson et al. 2010). Geomorphic and floristic class assignments for each plot were retained in 2018 as part of our analyses (see Analysis, below).

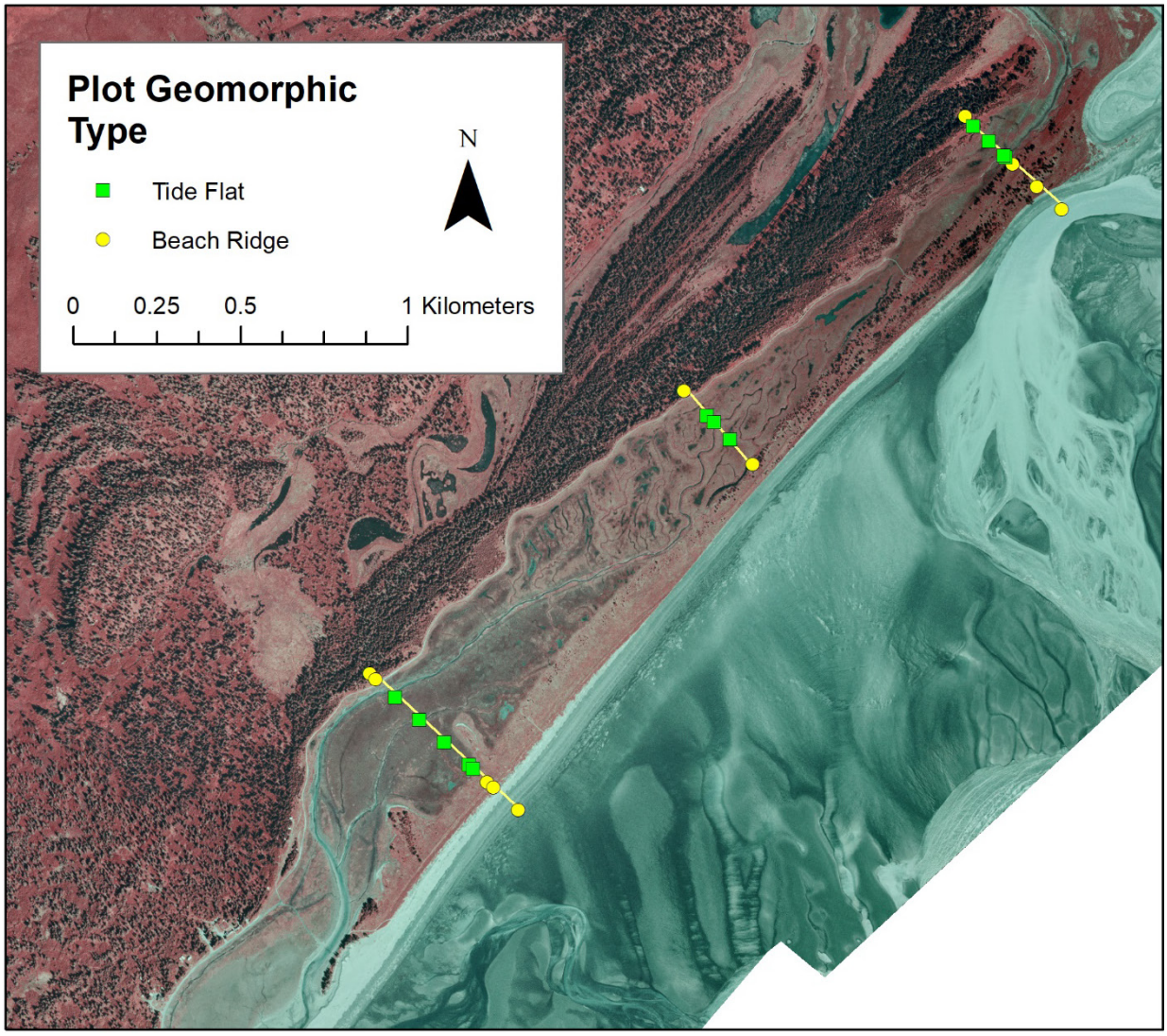

Figure 2. Distribution of Tidal Flat and Beach Ridge sample plots on three transects at Silver Salmon Creek, Lake Clark National Park & Preserve. Beach ridge communities range from those on the active foredunes and barrier beaches, to those that are located in the upper marsh areas on abandoned beach ridges. Species composition in these two environments (active and abandoned beach ridges) often differ.

New monitoring sites were also established at three coastal marshes in KEFJ in August 2018: Beauty Bay, North Arm of Nuka Bay, and Long Beach in Northwestern Fjord (Figure 1). Monitoring plots

were established using the same methods as in LACL and KATM salt marshes (Jorgenson and Miller 2010), with the following modifications: (1) plot-to-plot spacing was reduced to 50m intervals, and transect-to-transect spacing likewise reduced due to the small size of the sites in KEFJ; and (2) plots in KEFJ were established on the right (south or west) side of each transect, looking down the transect from 0m to the water.

List 1. Floristic classes recorded at monitoring sites in 2007 and 2008, from Jorgenson et al. (2010). Where taxonomic names have changed, the current nomenclature is shown first, followed by the original class name used in Jorgenson et al. (2010). Appendix B includes current nomenclature for all taxa recorded in 2018.

- *Carex lyngbyaei-Calamagrostis deschampsioides*
- *Carex glareosa-Carex ramenskii*
- *Lathyrus maritimus-Senecio pseudoarnica*
- *Carex ramenskii-Stellaria humifusa*
- *Leymus mollis-Plantago maritima = Elymus mollis-Plantago maritima* (2010)
- *Achillea millefolium-Carex gmelinii*
- Barren Beach
- *Carex lyngbyei-Cicuta virosa*
- *Hippuris tetraphylla-Triglochin maritimum*
- *Calamagrostis canadensis-Lupinus nootkatensis*
- *Leymus mollis-Carex lyngbyei = Elymus mollis-Carex lyngbyaei* (2010)
- Barren Mudflat
- *Calamagrostis canadensis-Equisetum fluviatile*
- *Myrica gale-Salix fuscescens*
- *Hippuris vulgaris-Sparganium angustifolium*
- *Alnus sinuata-Dryopteris dilatate*
- *Picea sitchensis-Angelica lucida*
- *Carex mackenziei-Eleocharis kamtschatica*

Analysis

To determine whether community composition had changed across years, we examined only plots visited in both years. To assess vegetation changes within geomorphic groups or entire sites, we analyzed only systematically-located study plots. When assessing vegetation change in floristic classes, we included subjectively-located plots, as these were sampled in 2007–2008 to capture under-represented vegetation types.

Cover of All Vascular Plants, Functional Groups, and Individual Species

To assess changes in the summed cover of all vascular species, changes in the summed cover of selected functional groups, and changes in cover of individual species, we developed a generalized linear mixed effects model (GLMM) of point-intercept data. Because of the potential for misidentification of low-stature sedge species that occurred in the grazed meadows, we grouped several species of *Carex (Carex ramenskii, C. pluriflora, C. mackenziei, C. glareosa)* and analyzed their summed cover for each plot. We also analyzed the summed plot cover of tidal flat bear forage species *(Carex ramenskii, C. pluriflora, C. mackenziei, C. glareosa, Triglochin maritimum, T. palustris, Plantago maritimum)*, beach ridge bear forage species (*Angelica lucida, Angelica genuflexa, Lupinus nootkatensis*), halophytic species (*Triglochin maritimum, Triglochin palustris, Plantago maritima, Puccinellia phrygenodes, Puccinellia nuttallii, Stellaria humifusa, Carex ramenskii*), and all grasses, deciduous shrubs, sedges, forbs. Lastly, we applied the GLMM to the cover of eight individual species of interest: *Elymus mollis, Festuca rubra, Picea sitchensis, Carex ramenskii, Myrica gale, Salix fuscescens, Salix barclayii,* and *Carex lyngbyei.*

The number of hits for a species or functional group in a plot was modeled with a binomial error distribution and a logit link (species) or a Poisson error distribution and a log link (functional groups).The probability (binomial model) or rate (Poisson model) parameter estimated in our models is our estimate of cover for the species or functional group. We modeled random effects for plot intercepts and slopes, nested within plot-blocks. We made inference from this model in a Bayesian framework and summarized parameter estimates and other model-derived quantities as posterior means and 95% credible intervals. A detailed model description is presented in Appendix C. Because these results were extrapolated to characterize changes across all study sites in LACL and KATM, we limited our dataset to systematic plots to ensure a representative sample. We used the jagsUI (Kellner 2018) package in R (R Core Team 2019) and JAGS (Plummer 2017) to perform this model analysis.

Community Composition

To examine changes in species composition through time, we used a subset of our data consisting only of plots that were visited during both sampling events. We visualized multivariate patterns using Non-Metric Multidimensional Scaling (NMDS), performed using the vegan package (Oksanen et al. 2019) in the R statistical computing environment (R Core Team 2019). NMDS was performed with a Bray-Curtis dissimilarity measure on raw point-intercept counts. We used PERMANOVA (Anderson 2001) and PERMDISP (Anderson 2017) to test for differences in multivariate species space between the 2007–2008 and 2018 sampling events, as well as between geomorphic classes and among floristic classes. Our primary objective was to characterize changes in species composition and cover through

time, but to better understand the relative magnitude of temporal changes, and to allow for changes to vary among geomorphic and floristic classes we included those groups in our analyses. PERMANOVA is sensitive to differences in both the multivariate centroid (the average species composition for a group) and the dispersion around that centroid (plot-to-plot differences in species composition within the group, known as β-diversity). PERMDISP tests for differences in β-diversity (dispersion) among groups. In practice, these two analyses were used together to understand differences in the average species composition and differences in β-diversity between years, geomorphic groups and floristic classes. We used a Bray-Curtis distance measure calculated from species cover (hits / number of points surveyed) and from proportional composition (hits / total plot hits) for both PERMANOVA and PERMDISP.

PERMANOVA calculates sums of squares from a distance matrix calculated from the species-by-site table. F-values are calculated from the sums of squares as in a traditional ANOVA, but significance is assessed by permuting the data many times to generate a population of F-values under the null hypothesis. The observed F-value is then compared to this population to derive a p-value. Different permutation schemes are required to test different hypotheses, with the conceptual guide being to permute objects that should be exchangeable under the null hypothesis. So to test whether communities differed between sampling occasions we permuted observations within plots but not among plots, because our null hypothesis of no change in time would lead to observations that are exchangeable in time, but we would still expect differences among plots. Conversely, to test whether community composition varied between geomorphic classes, we permuted plots, holding observations within them constant, effectively disassociating geomorphic group values from observations while maintaining the structure imposed by the spatial layout of our data collection. We also tested whether composition differed among floristic classes, and for interactions between floristic class × sampling event, and geomorphic class × sampling event. The same permutation designs were used with PERMDISP analyses. We structured our PERMANOVA analysis as a split-plot design with observations nested within plots, plots nested within transects, and sites serving as blocks. PERMANOVA and PERMDISP were performed using the vegan package (Oksanen et al. 2019) in the R statistical computing environment (R Core Team 2019) .

To explore whether changes in species composition were pronounced enough to result in changes in floristic classes, we classified 2018 data using random forest. We trained a random forest model ensemble on 2008 data, fitting plot floristic classes with species composition data. Our random forest ensemble comprised 50 trees, each predicting floristic class using 20 randomly-chosen species. These parameters were chosen after examining out-of-bag error for random forests with a range tree and predictor variable numbers. Due to the small size of our data set, especially for some floristic classes, we did not separate training and validation data. The random forest ensemble was then used to predict the floristic class for all 2018 vegetation plots, including newly established plots in KEFJ. The out-of-bag misclassification rate of our random forest (fit to 2007–2008 data) was 29%, but by-class errors ranged from 0% to 100%. Generally, classes with few measured plots were poorly classified. To assess how meaningful any particular change in floristic classification was, we examined the out-of-bag error rate for that class (E), the classes into which plots in that floristic class were erroneously classified, and the proportion of trees that voted for the most popular class (Pv).

Post-hoc Analyses of Growing Season Conditions

To explore whether growing degree days (GDD), a cumulative heat index, may have contributed to the increase in vascular plant cover that we observed in 2018 relative to 2007–2008, we generated two relevant datasets. We calculated GDD using a base temperature of 5˚ C for 2007–2018 using data from King Salmon, Alaska, acquired from the National Centers for Environmental Information (https://www.ncdc.noaa.gov/cdo-web/; accessed April 24, 2020). First, we generated a daily temperature summary from the daily minimum and maximum temperature: $T_{avg} = T_{min} + T_{max}/2$. Then, we calculated GDD as a cumulative sum of the preceding daily summaries that were greater than 5˚ C. We also summarized estimated start of season (SOS) dates from MODIS NDVI seasonal metrics data (http://www.gina.alaska.edu/projects/modis-derived-ndvi-metrics) over the footprint of the Hallo Bay meadow complex.

Methodological Checks — Sampling Intensity

Because the sampling intensity within plots was reduced by half in 2018, from 100 sampled points per plot in 2007–2008 to 50 points in 2018, we examined the efficiency of both sampling intensities at capturing the species composition of the plot. To do so, we examined species accumulation curves for each plot using the vegan package (Oksanen et al. 2019) in R (R Core Team 2019), comparing 2007–2008 curves to 2018 curves. Generally, the reduced sampling intensity accumulated species at a similar rate as the original sampling and yielded similar species richness estimates. Rare species may not have been well sampled by either sampling intensity (Appendix A).

Results & Discussion

Plant communities appear to have remained relatively stable, overall, between 2007–2008 and 2018 sampling events: the variation in community composition between years was less than one tenth of the variation among floristic classes and less than one third of the variation between geomorphic groups (Table 1). The floristic classes identified in 2007 and 2008 accounted for 47% of the variation in community composition, and geomorphic group accounted for 17% (Table 1). Despite the relative stability in composition, we measured higher cover of vascular plants in 2018 than in 2007–2008 (Figure 3) and documented localized changes in species composition that translated into changes from one floristic class to another. These changes in floristic class tended to result from rapid colonization of beach dunes and mudflats, expansion of spruce cover, and shrub expansion at upper marsh margins. Many of these localized changes recorded in the plot data from 2007–2008 and 2018 are consistent with the changes reported by Jorgenson et al. (2010) in their comparison of images from the 1950s and early-mid 2000s. These changes included vegetation establishment on barren substrates (e.g., beach berms), drying and infilling of ponds, and expansion of spruce cover on outer beach ridges. Our field data from 2018 likewise showed rapid colonization of beach dunes and mudflats, increases in spruce cover, and expansion of shrubs at upper meadow margins. For example, the roughly 6% increase in coastal gravelly saline barrens reported in 2010 (Jorgenson et al. 2010) had provided new substrate for the expansion of beach ridge communities by 2018. Many of the changes we recorded in species composition occurred in plots at the margins (upper and lower) of the salt marsh communities.

Table 1. PERMANOVA of species composition based on cover (species hits/number of sample points) for sites sampled in both intervals. P-values reflect significance in a test for no difference in species composition among levels of the identified factor. PERMANOVA is sensitive to differences in both the multivariate centroid and dispersion. Geomorphic group refers to Beach Ridge and Tidal Flat environments; floristic classes are described by Jorgenson et al. (2010). A dash (–) indicates no data for the cell.

Model Term	df	SS	MS	F	R^2	p
Geomorphic Group	1.00	3.40	3.40	33.06	0.17	0.001
Floristic Class	12.0	9.31	0.78	7.53	0.47	0.001
Plot ID	14.0	2.97	0.21	2.06	0.15	0.999
Sampling Event	1.00	0.77	0.77	7.47	0.04	0.001
Geomorphic Group × Sampling Event	1.00	0.29	0.29	2.81	0.01	0.007
Floristic Class × Sampling Event	12.00	1.82	0.15	1.48	0.09	0.048
Residuals	14.00	1.44	0.10	–	0.07	–
Total	55.00	20.01	–	–	1.00	–

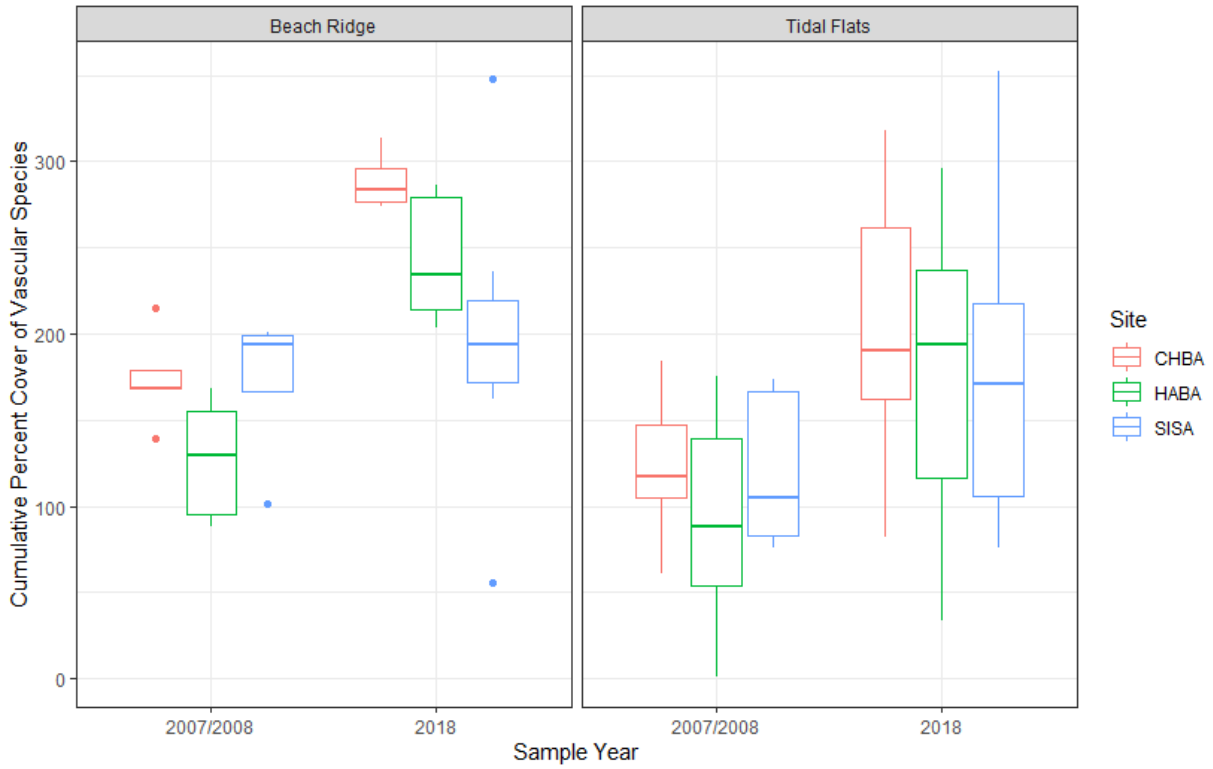

Figure 3. Total cover of vascular plants in 2007–2008 and 2018 on Beach Ridges and Tidal Flats at Chinitna Bay (CHBA), Hallo Bay (HABA) and Silver Salmon Creek (SISA). Boxplots show the median inside a box that spans the interquartile range (25th to the 75th percentile). Whiskers extending from the box to the largest observation that doesn't exceed 1.5 × the interquartile range. More extreme values are plotted as points.

Changes in Total Vascular Plant Cover

Cover of vascular species was greater in 2018 than in 2007–2008, increasing from 118% [114–121] to 183% [177–189] (posterior mean with 95% credible interval, Table 2, Figure 3). The increase in cover was consistent across monitoring sites (Figure 3) and across most floristic classes (Figure 4).

Table 2. GLMM results showing observed and modeled mean cover (+/− 95% CrI), and differences in cover for species and functional groups in 2007–2008 and 2018. R̂ is the Gelman Rubin statistic for Markov chain monte carlo convergence, for which values closer to one are better, and values less than 1.1 indicate convergence.

	2007/8 Cover			2018 Cover			Difference			
Species or Group	Posterior Mean	Lower 95% CrI	Upper 95% CrI	Posterior Mean	Lower 95% CrI	Upper 95% CrI	Posterior Mean	Lower 95% CrI	Upper 95% CrI	R̂
LEYMOLM	0.099	0.093	0.105	0.170	0.163	0.178	0.072	0.062	0.082	1.005
FESRUB	0.061	0.056	0.066	0.193	0.184	0.201	0.132	0.122	0.142	1.003
PICSIT	0.012	0.010	0.015	0.025	0.021	0.028	0.013	0.008	0.017	1.021
CARRAM	0.058	0.053	0.063	0.068	0.062	0.073	0.010	0.002	0.017	1.028
MYRGAL	0.035	0.031	0.038	0.045	0.040	0.049	0.010	0.004	0.016	1.029
SALFUS	0.035	0.031	0.038	0.038	0.034	0.043	0.004	−0.002	0.009	1.009
SALBAR	0.000	0.000	0.001	0.005	0.004	0.007	0.005	0.004	0.007	1.050
CARLYN	0.092	0.087	0.097	0.140	0.134	0.147	0.049	0.040	0.057	1.009
Bear Forage	0.162	0.148	0.177	0.343	0.319	0.368	0.181	0.152	0.210	1.039
Beach Bear Forage	0.050	0.042	0.058	0.052	0.043	0.062	0.003	−0.009	0.015	1.016
Small Sedges	0.113	0.102	0.125	0.171	0.154	0.188	0.057	0.036	0.078	1.013
Halophiles	0.144	0.130	0.157	0.278	0.256	0.301	0.135	0.109	0.161	1.073
Grasses	0.327	0.307	0.348	0.638	0.605	0.672	0.310	0.272	0.350	1.011
Forbs	0.481	0.457	0.506	0.699	0.664	0.734	0.217	0.175	0.260	1.088
Deciduous Shrubs	0.099	0.088	0.110	0.092	0.079	0.105	−0.007	−0.024	0.010	1.088
All Sedges	0.244	0.227	0.262	0.375	0.350	0.401	0.131	0.100	0.162	1.042
All Vascular	1.175	1.137	1.213	1.829	1.773	1.886	0.654	0.586	0.722	1.010

Figure 4. Total cover of vascular plants in 2007–2008 and 2018 across monitoring sites at Chinitna Bay (CHBA), Hallo Bay (HABA), and Silver Salmon Creek (SISA), by floristic classes assigned in 2007–2008. Floristic class names reflect taxonomy used in Jorgenson et al. (2010). Updated nomenclature is shown in Appendix B. Boxplots show the median inside a box that spans the interquartile range (25th to the 75th percentile). Whiskers extending from the box to the largest observation that doesn't exceed 1.5 × the interquartile range. More extreme values are plotted as points.

Changes in Cover of Functional Groups and Species

We found an increase in the cover of plants known to be foraged by coastal brown bears (Rode et al. 2001; Smith & Partridge 2004), as indicated by the GLMM results. The summed cover of several of these sedges *(Carex ramenskii, C. pluriflora, C. mackenziei, C. glareosa)* and salt-tolerant forbs *(Triglochin maritimum, T. palustris, Plantago maritimum)*, increased from 16.2% [14.8–17.7] in 2007–2008 to 34.3% [31.9–36.8] in 2018 (Figure 5, Table 2). Although these forage species nearly doubled in cover between the two sampling events, they did not comprise a greater proportion of the total cover within the plots where they were found (Figure 6).

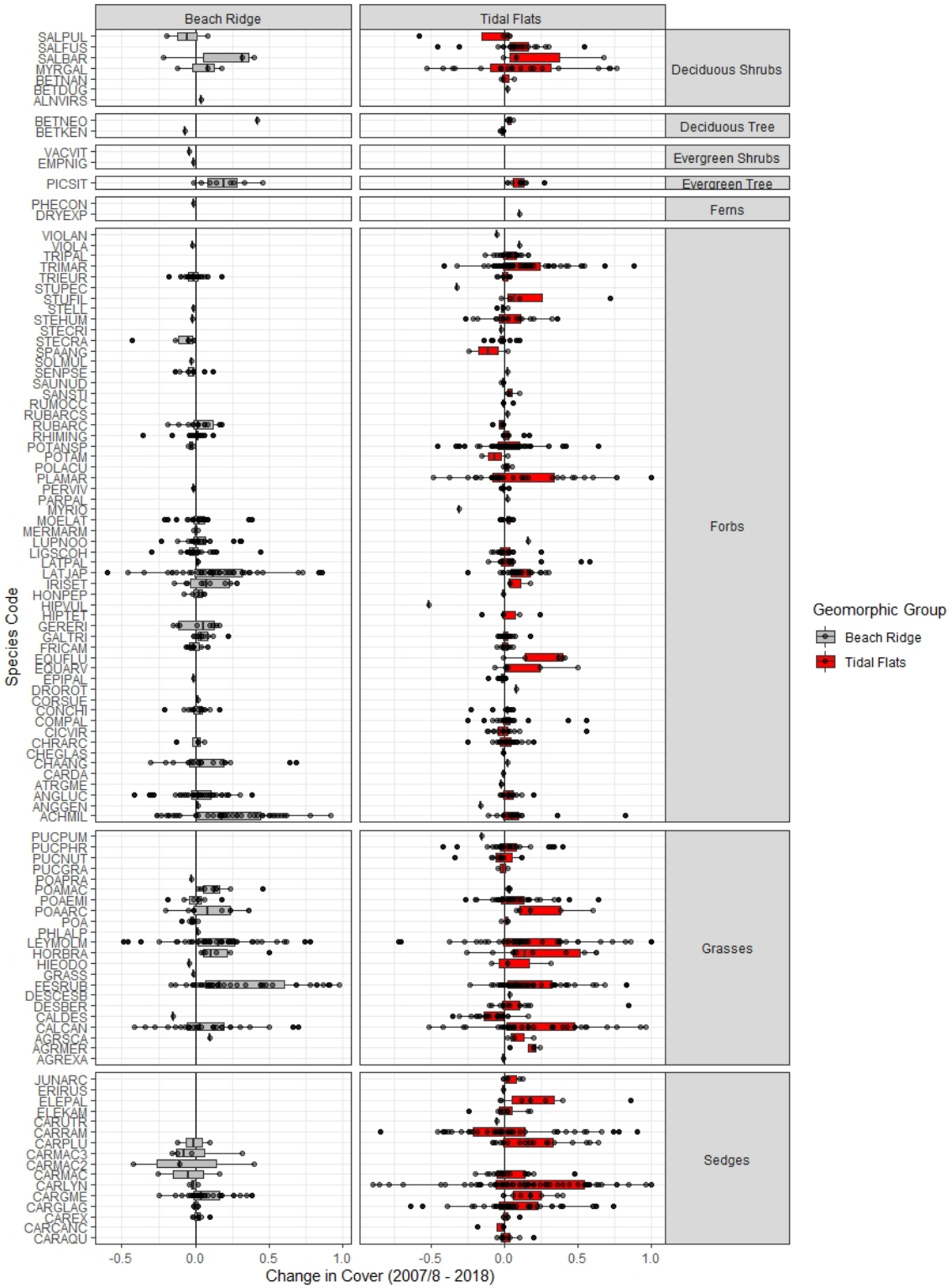

Figure 5. Change in per species cover (hits / number of points surveyed) between 2007–2008 and 2018 from raw point intercept data. Each dot is the change in cover of that species at a particular plot. Boxplots show the median inside a box that spans the interquartile range (25th to the 75th percentile). Whiskers extend to the largest value that doesn't exceed 1.5 × the interquartile range.

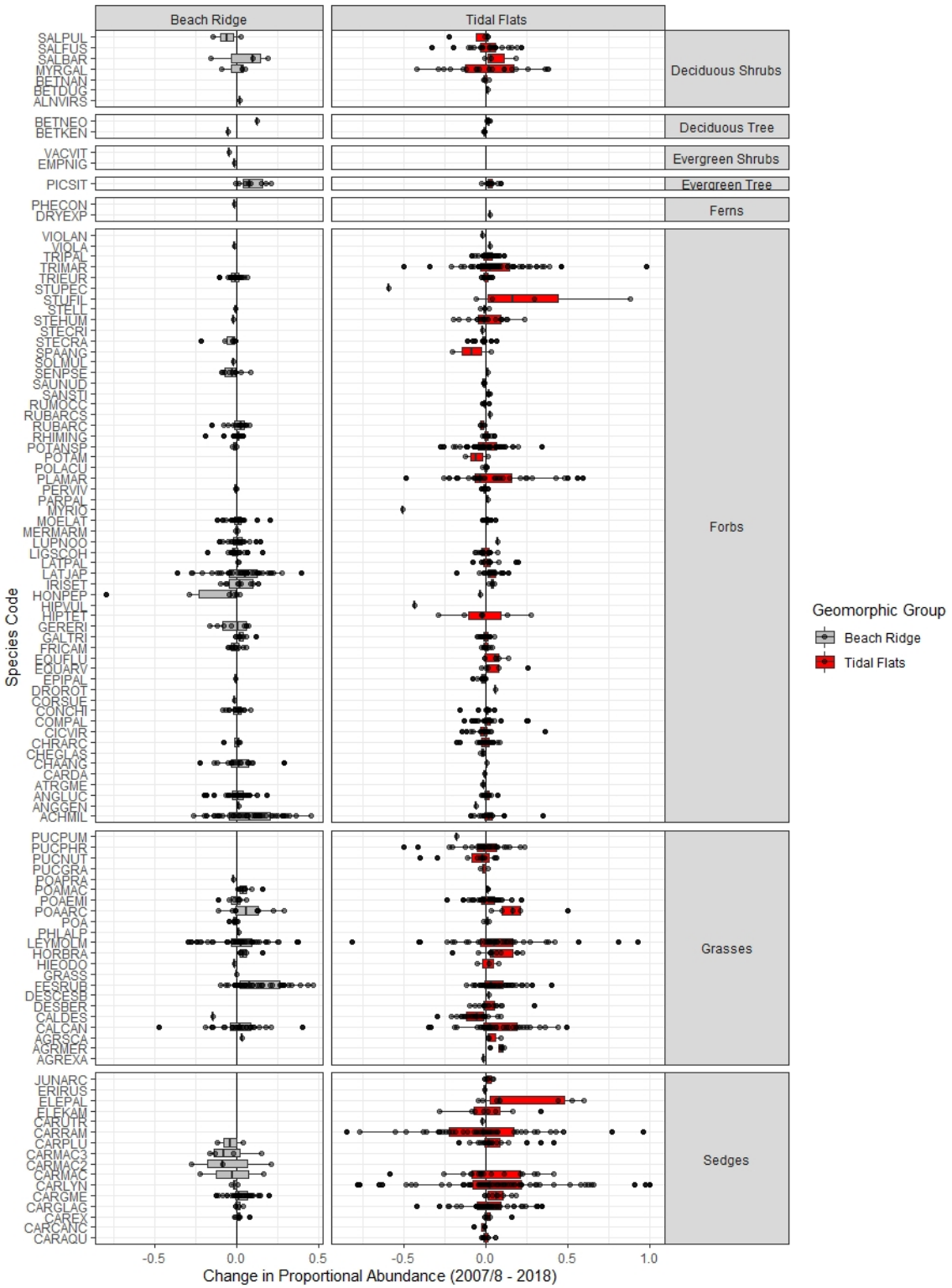

Figure 6. Change in per species proportion composition (hits / total hits) between 2007–2008 and 2018. Each dot is the change in proportional composition of that species at a particular plot. Boxplots show the median inside a box that spans the interquartile range (25th to the 75th percentile). Whiskers extend to the largest value that doesn't exceed 1.5 × the interquartile range.

Grasses showed the greatest increases in cover over the 10-year period between sampling events (Figure 5; Table 2). Total red fescue (*Festuca rubra*) cover increased from 6% [5.6–6.6] to 19% [18.4–20.1] and was observed in 8 more plots in 2018 than in 2007–2008, moving from the species with 4th highest total cover to highest total cover and remaining the most ubiquitous species at the plot scale (see Appendix D, Table D-1). Plots newly colonized by *F. rubra* were found in tidal flats and on beach ridges, and the two most dramatic increases among newly colonized plots were in the *Carex lyngbyei-Cicuta virosa* floristic class. Other substantial increases in *F. rubra* cover were found in *Leymus mollis-Carex lyngbyei, Myrica gale-Salix fuscecens, Calamagrostis canadensis-Lupinus nootkatensis, Leymus mollis-Plantago maritima, Picea sitchensis-Angelica lucida* and *Carex glareosa-Carex ramenskii* floristic classes. At plots where it was found, the average cover of *F. rubra* increased from 11% to 32%. Beach rye (*Leymus mollis*) cover increased from 10% [9.3–10.5] in 2007–2008 to 17% [16.3–17.8] in 2018 and was found at 9 new plots in 2018. Substantial increases in *L. mollis* cover were seen in plots of Barren Beach, *Calamagrostis canadensis-Lupinus nootkatensis, Carex glareosa-Carex ramenskii,* and *Achillea millefollium-Carex gmelinii* floristic classes. The *C. glareosa-C. ramenskii* meadow in which *Leymus* established was found at the meadow margin at the north end of Silver Salmon Creek.

Picea sitchensis/*P.* x *lutzii* increased from 1.2% [1.0–1.5] overall cover to 2.5% [2.1–2.8], and was found in 2 additional plots in 2018, in the *Leymus mollis-Carex lyngbyei* floristic class. Locally, the effect of increased growth in spruce was more pronounced: at plots where it was found, its cover increased from 6% to 23%. *Carex lyngbyei* cover increased from 9.2% [8.7–9.7] to 14.0% [13.4–14.7] across all plots. Sweetgale (*Myrica gale)*, a species indicative of moist, acidic soils, increased from 3.5% [3.1–3.8] to 4.5% [4.0–4.9] cover between the two sampling events (Table 2, Figure 5).

Seasonal increases in aboveground biomass cannot fully account for the widespread increases in cover that we recorded between 2007–2008 and 2018, but they may have contributed to it. At Silver Salmon Creek, most sites were sampled twice in 2018: once in early June, corresponding to the 2007 sampling dates, and once in early September, when biomass would have been at a maximum for the year. Total cover measured in June 2018 was comparable to cover measured at the site in June 2007 but cover in September 2018 was higher than in June of either year. Likewise, we saw an increase in cover at Chinitna Bay, where plot measurements in 2018 occurred a month later than they had in 2007. In both cases, the increases in cover associated with sampling dates later in the summer indicated that seasonality may have affected our measurements. At Hallo Bay, however, the increase in cover appeared to be independent of timing: we sampled plots within the same date range (mid-July) in 2008 and 2018, but still recorded an increase in cover in 2018.

There are several other possible explanations, beyond the delayed sampling at the Lake Clark sites, for the increases in cover that we found across all sites between 2007–2008 and 2018. Growing degree days have been shown to be a strong predictor of primary productivity in Arctic ecosystems (e.g., Karlsen et al. 2018), and we found that a greater number of growing degree days (GDD) had accumulated by the start of sampling in 2018 than in either 2007 or 2008 (Figure 7). The first year of sampling in Hallo Bay, 2008 had the lowest accumulation of GDD of any year in our record (2007–2018; Figure 7), and cumulative GDD by mid-July (Day 197) had increased by approximately one-

third between 2008 and 2018. The increase in cumulative GDD between 2007 and 2018 could have contributed to the increase in cover (a proxy for plant biomass) that we recorded over the last decade. Increases in graminoid and shrub biomass, in particular, have been cited in response to warming across the Arctic, often attributed to increases in soil nutrient availability (e.g., Hill & Henry 2011; Villarreal et al. 2012; Fraser et al. 2014).

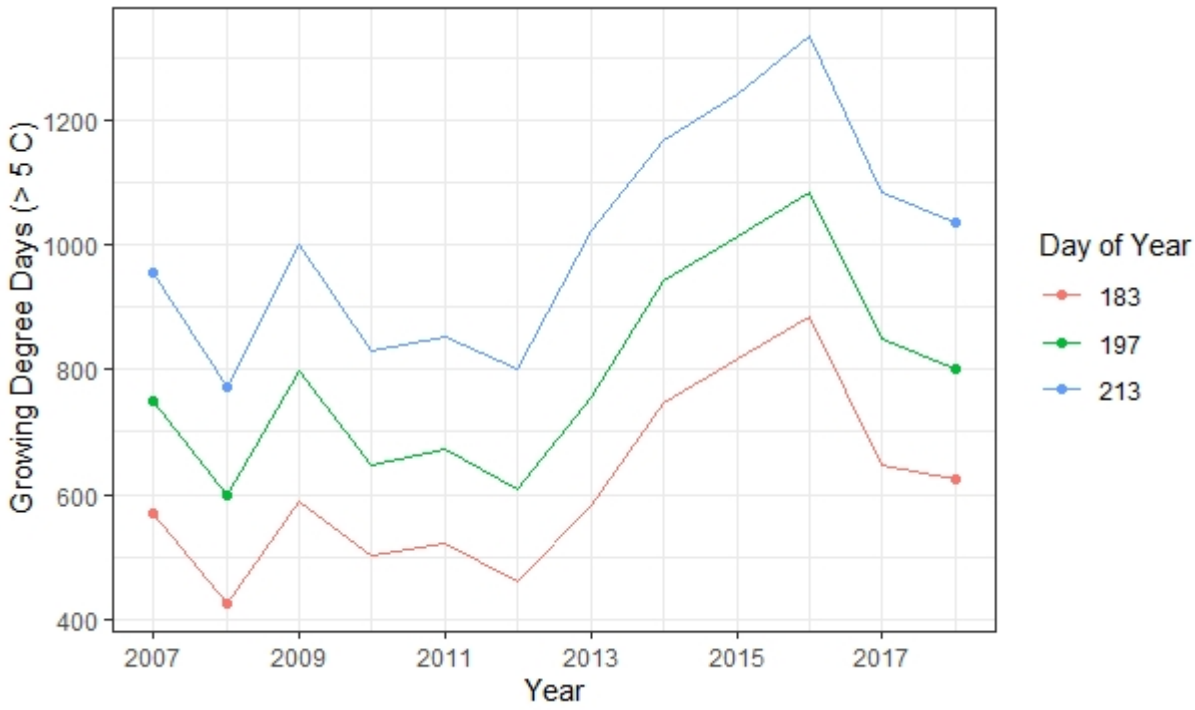

Figure 7. Cumulative growing degree days (base 5 degrees C) at the King Salmon, Alaska, airport through the month of July (2007–2018). Points mark the years of vegetation sampling (2007, 2008, 2018). Day of year is equivalent to July 2 (Day 183); July 16 (Day 197); and August 1 (Day 213) in non-leap years.

Alternatively, an earlier start of the growing season in 2018 could have contributed to the observed increase in cover; i.e., green-up dates estimated from Moderate Resolution Imaging Spectroradiometer (MODIS) data for Hallo Bay indicate that mean green-up occurred roughly 10 days earlier in 2018 than in 2008 (M. Hannam, unpublished data).

Lastly, it is possible that the different point-intercept measurement methods (laser vs. pin-drop) used during the 2007–2008 and 2018 sampling events resulted in higher cover estimates in 2018 than in the previous years. Laser-pointer dots can be difficult to see in some lighting conditions, which could have led to a systematic underestimation of cover in 2007–2008. Conversely, the tip of the pin may have been interpreted as larger in cross section than the laser dot, leading to systematic overestimation of cover in 2018.

Changes in Community Composition

Geomorphic setting was an important determinant of plant communities in salt marshes of Lake Clark and Katmai National Parks & Preserves. Nearly one-fifth the variation in species cover (PERMANOVA, 17%, p =.001; Table 1) and composition (PERMANOVA, 19%, p =.001; see Appendix D, Table D-2) was explained by geomorphic class (Beach Ridge versus Tidal Flat), and nearly one half explained by floristic class (PERMANOVA, 47%, 49% respectively, p =.001). The geomorphic separation in species-space was likewise evident in the ordination (Figure 8). Species composition and cover varied more among plots in tidal flats than on beach ridges (PERMDISP, p=.001, nperms = 999).

Species composition in monitoring plots changed between sampling events (Table 1), and the nature of the change varied among floristic classes and geomorphic groups. Changes in species composition through time were small relative to variation among geomorphic groups or floristic classes; i.e., changes between 2007–2008 and 2018 accounted for less than 10% of the variability in species cover or composition (Table 1). In some cases, compositional change was detectable as a change in floristic class (Table 3). Such changes were more difficult to detect in rarer floristic classes, due to smaller sample sizes and greater error rates.

The NDMS ordination provided a fair to good representation of plots in two dimensions (stress=0.13). The first NMDS axis largely corresponded to plot elevation and electrical conductivity, an indicator of salinity (Figure 8). Among beach ridge plots, the second NMDS axis appeared to separate early successional from later successional communities, but among tidal flat communities, the second axis was not easily attributable to plot covariates.

Across all sites, the most ubiquitous species in 2018 included the beach ridge dominants *Festuca rubra*, *Leymus mollis, Lathyrus japonicus, Achillea millefolium, Angelica lucida, Carex gmelinii*, and *Ligusticum scoticum* (see Appendix D, Table D-1). *Carex lyngbyei*, a species found along tidal guts and in brackish and freshwater wetlands, was also recorded in a high proportion of plots.

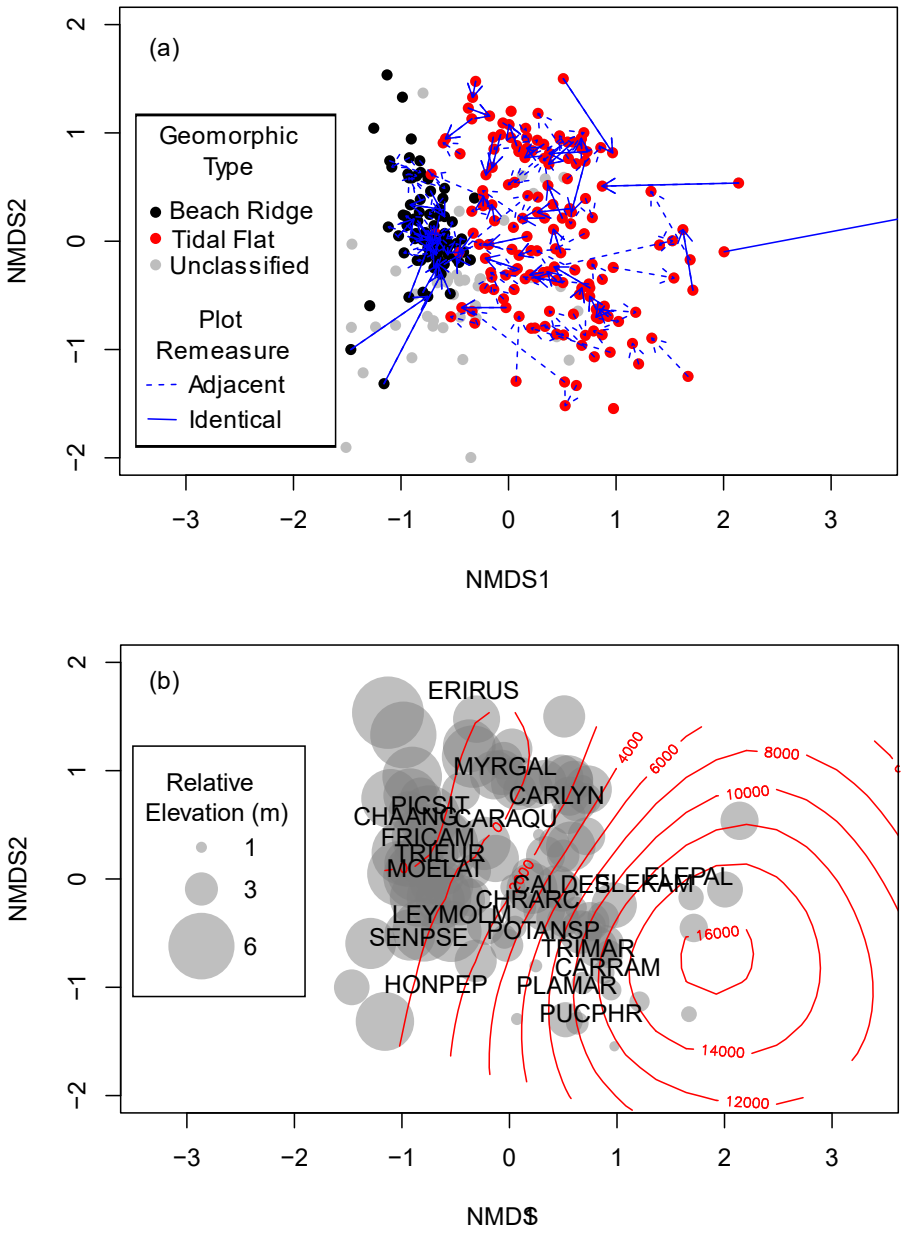

Figure 1. Non-metric multidimensional scaling (NMDS) of salt marsh monitoring plots in species space. (a) Change from 2007–2008 to 2018 is indicated for replicate plots (solid arrows) and plots in the same plot-block (dashed arrows) for beach ridge (black), tidal flat (red), and unassigned geomorphic groups that were only measured in 2018 (gray). (b) Species centroids and environmental attributes shown for reference (species codes in Appendix B). Plot point sizes are scaled to plot elevation, and contour lines are fit to electrical conductivity measured at plots in 2007 and 2008. Figures have been cropped to show detail and exclude five plots. Plot distribution of beach ridge species is narrower than that for tidal marshes, the latter of which occupies a broader environmental range in terms of elevation, salinity, and soil moisture.

Table 1. Results of random forest classification of monitoring plots. Rows show floristic classes assigned in 2007–2008 by Jorgenson et al. (2010). Columns show floristic classes assigned in 2018. Table cells show the number of plots assigned to a given class, and the classification error based on out-of-bag samples in the 2007–2008 data. A dash (–) indicates no data for the cell.

Floristic Class	*Achillea millefolium-Carex gmelinii*	*Alnus sinuata-Dryopteris dilatata*	*Barren Mudflat*	*Calamagrostis canadensis-Equisetum fluviatile*	*Calamagrostis canadensis-Lupinus nootkatensis*	*Carex glareosa-Carex ramenskii*	*Carex lyngbyaei-Calamagrostis deschampsioides*	*Carex lyngbyaei-Cicuta virosa*	*Carex mackenziei-Eleocharis kamtschatica*	*Carex ramenskii-Stellaria humifusa*	*Elymus mollis-Carex lyngbyaei*	*Elymus mollis-Plantago maritima*	*Estuarine Water*	*Hippuris tetraphylla-Triglochin maritimum*	*Lathyrus maritimus-Senecio pseudoarnica*	*Myrica gale-Salix fuscescens*	n	Classification Error rate
Achillea millefolium-Carex gmelinii	8	–	–	–	–	–	–	–	–	–	–	–	–	–	1	–	9	0.33
Barren Beach	–	–	–	–	–	–	–	–	–	–	–	–	–	–	2	–	2	0.00
Barren Mudflat	–	–	1	–	–	–	–	–	–	2	–	1	–	–	–	–	4	0.17
Calamagrostis canadensis-Equisetum fluviatile	–	1	–	2	–	–	–	1	–	–	–	–	–	–	–	–	4	0.75
Calamagrostis canadensis-Lupinus nootkatensis	–	–	–	–	10	–	–	–	–	–	–	–	–	–	–	–	10	0.25
Carex glareosa-Carex ramenskii	–	–	–	–	–	11	–	–	–	–	1	–	–	–	–	–	12	0.15
Carex lyngbyaei-Calamagrostis deschampsioides	–	–	–	–	–	1	3	1	–	–	–	–	1	–	–	–	6	0.43
Carex lyngbyaei-Cicuta virosa	–	–	–	–	–	1	–	9	–	–	–	–	–	–	–	–	10	0.00
Carex mackenziei-Eleocharis kamtschatica	–	–	–	–	–	–	–	–	3	–	–	–	–	–	–	1	4	0.50
Carex ramenskii-Stellaria humifusa	–	–	–	–	–	–	–	–	–	6	–	–	–	–	–	–	6	0.17
Elymus mollis-Carex lyngbyaei	1	–	–	–	1	–	–	1	–	–	–	–	–	–	1	–	4	0.75
Elymus mollis-Plantago maritima	–	–	–	–	–	–	–	–	–	–	–	5	–	–	–	–	5	0.40
Hippuris tetraphylla-Triglochin maritimum	–	–	–	–	–	1	–	–	–	–	–	–	–	1	–	–	2	0.67
Hippuris vulgaris-Sparganium angustifolium	–	–	–	–	–	–	–	1	–	–	–	–	–	–	–	–	1	1.00
Lathyrus maritimus-Senecio pseudoarnica	2	–	–	–	1	–	–	–	–	–	–	–	–	–	5	–	8	0.11
Myrica gale-Salix fuscescens	–	–	–	–	–	–	–	–	–	–	–	–	–	–	–	6	6	0.14
Picea sitchensis-Angelica lucida	–	–	–	–	–	–	–	–	–	–	–	–	–	–	1	–	1	1.00
n	11	1	1	2	12	14	3	13	3	8	1	6	1	1	10	7	94	–

Beach Ridge Succession

Species composition at our beach ridge plots became more similar (converged) through time, as indicated by a decrease in β-diversity among plots between sampling events (PERMDISP, Nperms=999, p = .004). This convergence appeared to be largely driven by succession: (1) colonization of barren beach at a few plots and the loss of a few outlier species (e.g., *Honckenya peploides*), and (2) a homogenization of beach ridge plots that became more similar in species composition. We are unable to say whether this shift in β-diversity was accompanied by a change in the average community composition on beach ridges, but the ordination results suggest a transition of early-successional beach ridge communities dominated by *Leymus mollis* and a few forbs to more species-rich assemblages (Figure 9). Vegetative colonization of coastal beach barrens was evident in the NMDS (Figure 8; Figure 9), repeat photos (Figure 10), and as the conversion from barren beach to the *Lathyrus japonica-Senecio pseudoarnica* floristic class in our random forest classification analysis (Table 3). Two of eight sites classified as *Lathyrus japonica-Senecio pseudoarnica* in 2007–2008 changed to the more species-rich *Achillea millefolium-Carex gmellinii* class in 2018 (Table 3). The increase in *Picea sitchensis*/*P.* x *lutzii* cover was manifest primarily in beach ridge plots (Figure 8).

The changes in species composition and cover that we found between 2007–2008 and 2018 in LACL and KATM are consistent with the widespread, multi-decadal changes reported in Jorgenson et al. (2010). The 1964 earthquake, which resulted in the conversion of active tidal flats (pre-1964) to inactive tidal flats (post-1964), and to the abandonment of beach ridges inland from the active beaches, has had a lasting effect on these ecosystems (Jorgenson et al. 2010). Erosion and accretion resulting from storm surges, tidal fluctuations and nearshore currents have resulted in longshore transport of sand and gravels near Glacier Spit, east of Chinitna Bay (Cusick & Bennet 2005), and have provided new substrate for beach ridge communities to expand seaward between 2007 and 2018. Conversely, erosion near the mouth of Johnson River at Silver Salmon Creek has cut into the adjacent beach ridge and removed established vegetation. Succession has led to increased cover in parts of beach ridges and inactive tidal flats, and an increase in Sitka/Lutz spruce cover as trees have matured and new individuals have established (Jorgenson et al. 2010).

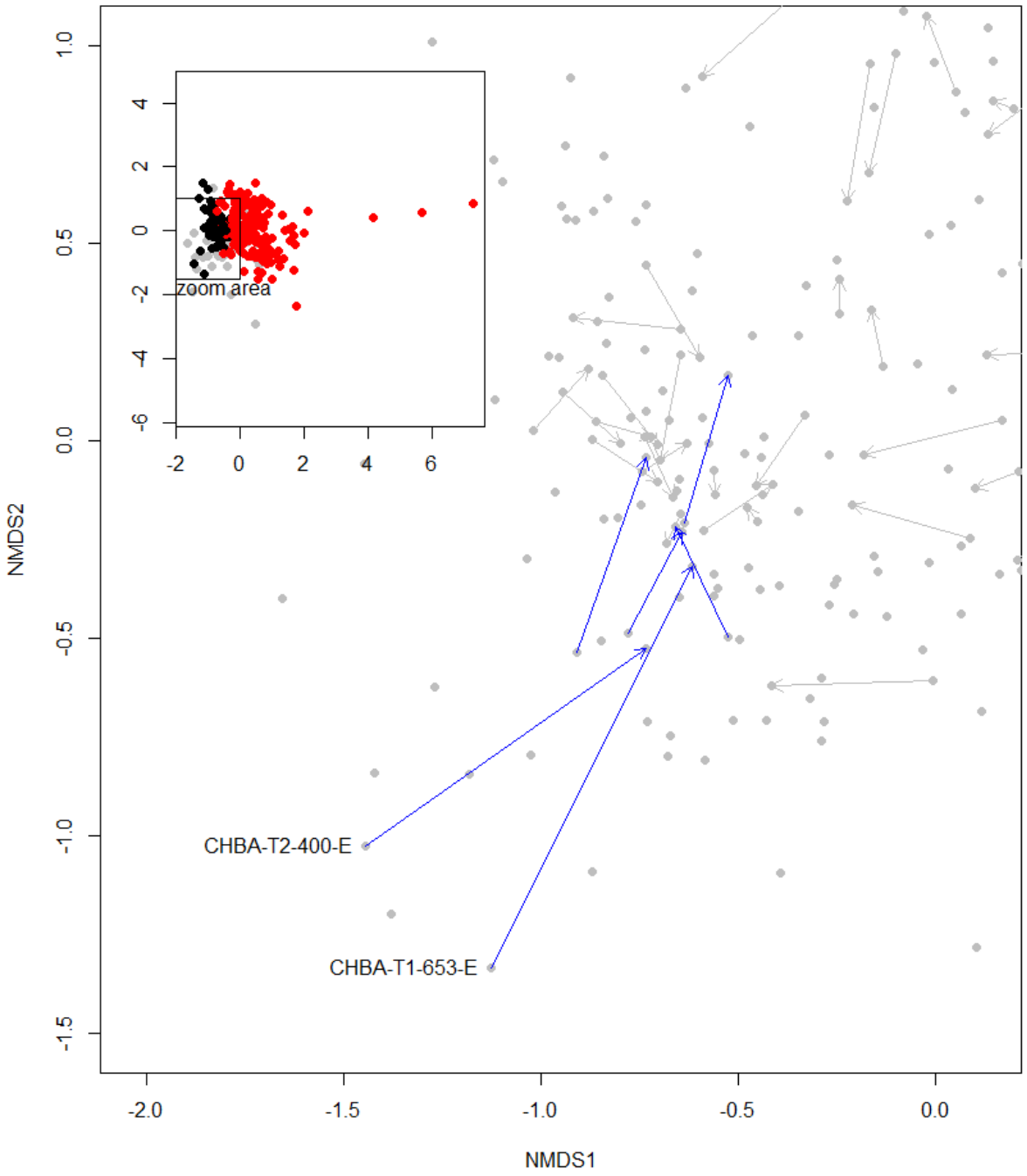

Figure 9. Beach ridge succession at six monitoring plots visualized in NMDS. Inset panel shows full NMDS graph with monitoring plots colored according to geomorphic group, tidal flat (red) or beach ridge (black), and zoomed extent of figure. Arrows point from 2007 vegetation to 2018 vegetation composition at re-measured plots. Labeled plots are pictured in Figure 10.

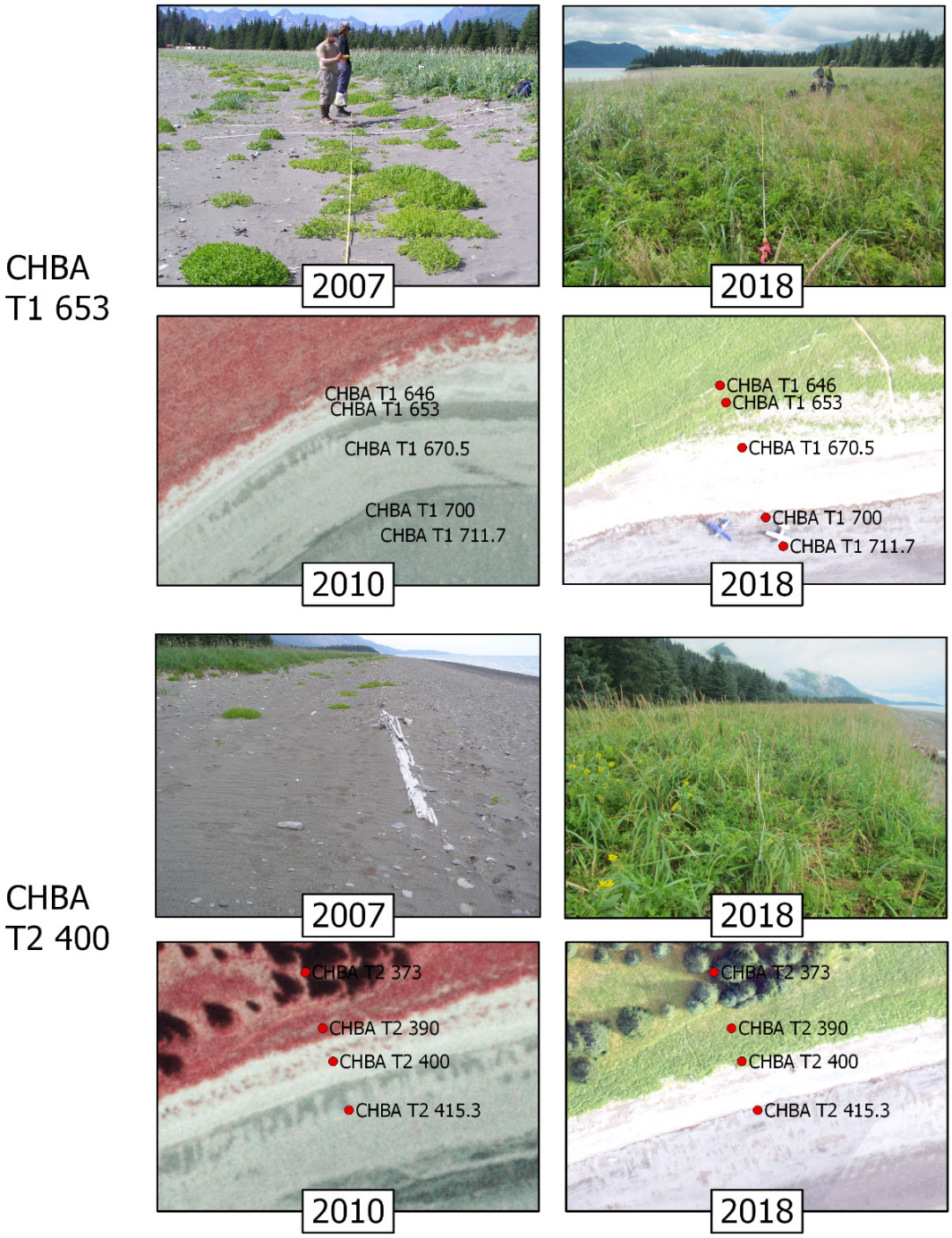

Figure 10. Beach ridge colonization and succession between 2007 and 2018 at two re-measured monitoring sites at Chinitna Bay. For each site, the top two panels show oblique photos of plot taken at the time of sampling and the bottom two panes show aerial photography of the plot vicinity taken during the sampling interval. In both cases, shoreline sediment deposition preceded colonization by *Honckeyna peploides*. Establishment of a suite of new species since 2007 has resulted in a diverse beach ridge assemblage.

Changes in Tidal Flat Communities

On tidal flats, community composition differed between sample visits. Because we detected a difference in community composition between sample events (Table 1) but no significant difference in β-diversity of tidal flat plots between sample events (PERMDISP, p =.703, nperm = 999), we performed a PERMANOVA on a subset of the species cover composed of only tidal flat plots sampled in both years. This revealed a significant difference in community composition between sample events (p=.001, Nperms = 999, see Appendix D, Table D-3).

NMDS revealed an overall shift towards communities indicative of lower salinity and higher elevation (Figure 8). Part of this shift was due to a colonization of mudflats by halophytic species. In Hallo Bay, two plots converted from barren mudflat to *Carex ramenskii-Stellaria humifusa* (HABA-T2-1000 and HABA-T2-1200) and *Leymus mollis-Plantago maritima* (HABA-T2-1000; Figures 11–12; Table 3), and additional plots appeared to follow similar trajectories (Figure 11). Similar patterns of mudflat colonization in the decades since the 1964 earthquake have been reported elsewhere in the upper Cook Inlet (Ulman et al. 2019). We also observed the colonization of formerly halophyte-dominated plots by less salt-tolerant species such as *Festuca rubra* (e.g., SISA-T2-200, Figure 8; Figure 11).

Transitions from halophytic to brackish communities in some locations were balanced by conversion of bare mudflat to halophyte communities in other locations. Post-hoc models (GLMM) of the cumulative cover and composition of 7 halophytic species (*Triglochin maritimum, Triglochin palustris, Plantago maritima, Puccinellia phrygenodes, Puccinellia nuttallii, Stellaria humifusa, Carex ramenskii*) revealed greater cover in 2018 (28% [26–29]) than in 2007–2008 (14% [13–15]) but a similar proportion of total vascular species cover (Table 2).

The draining and/or infilling of ponds reported by Jorgenson et al. (2006, 2010), recorded from aerial photos and satellite imagery between the 1950s and 2000s, was less apparent in our plot data. We observed increases in species cover of aquatic and/or wetland species (e.g., *Hippuris tetraphylla* and *Carex lyngbyei*; CHBA-T4-355) in one shallow pond between 2007–2008 and 2018, consistent with a pattern of drying and infilling, but due to limited sample size we were unable to detect a change in floristic class for the *Hippuris*-dominated plots (Table 3). Changes in surface hydrology can be dependent on weather and tides, and although we cite the examples above as evidence of successional changes in ponds and wet meadows, we also sampled plots that were more inundated in 2018 than in 2007–2008, presumably due to differences in tidal regime between years (CHBA-T2-100; HABA-T2-200; HABA-T2-700; HABA-T4-300, Figure 12).

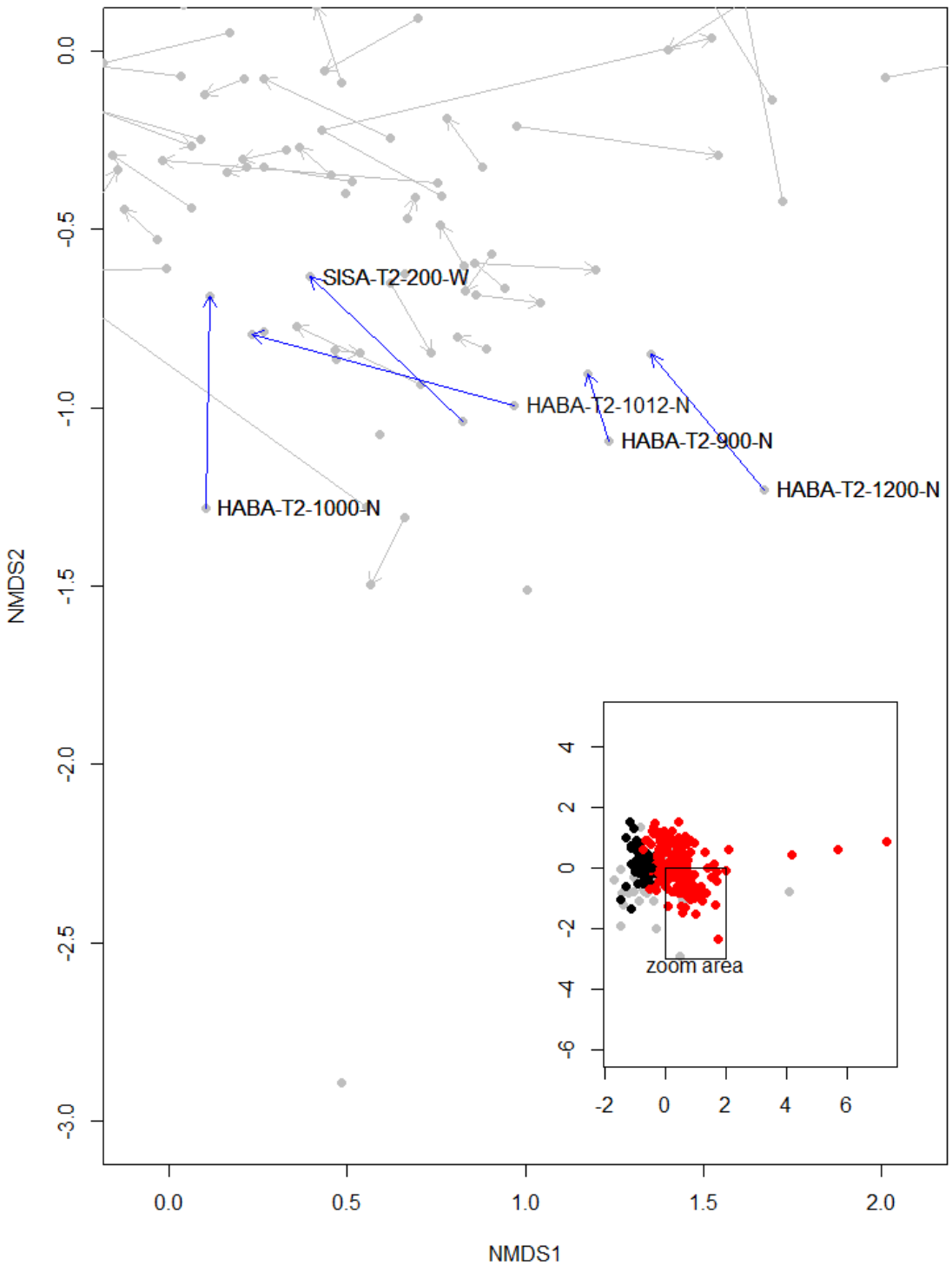

Figure 11. Mudflat colonization and halophyte to brackish transition at five monitoring plots visualized in NMDS. Inset panel shows full NMDS graph with monitoring plots colored according to geomorphic group, tidal flat (red) or beach ridge (black), and zoomed extent of figure. Arrows point from 2007–2008 vegetation to 2018 vegetation composition at re-measured plots.

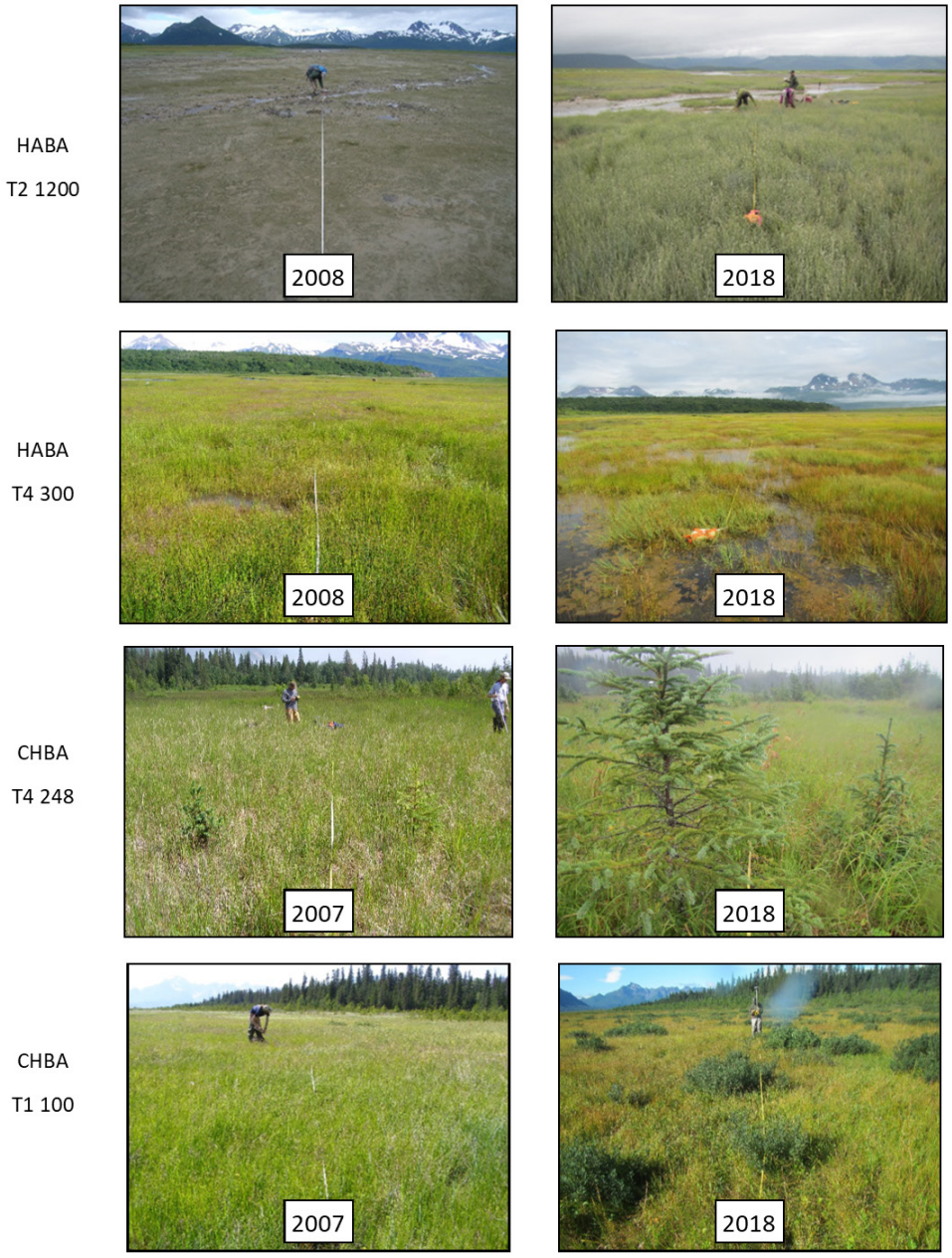

Figure 12. Photo pairs of initial and recent sampling of vegetation plots showing mudflat colonization at Hallo Bay (HABA-T2-1000); inundation of a wet meadow in 2018 (HABA-T4-300); rapid growth of spruce in a meadow that experienced uplift during the 1964 earthquake (CHBA-T4-248); and shrub (*Myrica gale*) colonization in an herbaceous meadow near the forest-marsh boundary (CHBA-T1-100).

We recorded changes in species composition at several sedge meadow plots (Figure 8). However, we didn't find evidence for broad-scale conversion of either *Carex ramenskii-stellaria humifusa* or *Carex glareosa-Carex ramenskii* to other floristic classes (Table 3), suggesting that the *C. ramenskii* meadow communities have remained relatively stable over the last decade. Shrub cover increased in at least two sedge meadow plots (CHBA-T1-100, CHBA-T1-41; Figure 12), leading to a change in

floristic class from *Carex lyngbeii-Calamagrostis deschampsoides* to *Myrica gale-Salix fuscecens* at one of the plots (CHBA-T1-41; Table 3.). The changes that we found in species composition in the *Carex* meadows tended to be localized to ecological margins (ecotones): for example, *Leymus mollis* established at the upper margin of a *Carex ramenskii* meadow at Silver Salmon Creek (SISA-T3-100); *Myrica gale* established in the upper margins of a *Carex* meadow in Chinitna Bay (CHBA-T1-100; CHBA-T1-41); and *Carex ramenskii* established on mudflats, at the lower margins of an existing meadow system in Hallo Bay (HABA-T2-1000; HABA-T2-1200; Figure 11).

Ecotones, or the transition zones between communities, may be particularly responsive to environmental change when species are living near the edge of their tolerances (Peters et al. 2006). The increases in cover of several species (e.g. *Leymus mollis*, *Myrica gale*, *Carex ramenskii*) in the upper and lower meadow margins suggest that we may see the greatest change in species composition occurring around the edges of the existing meadow systems. Here, as in other studies (e.g. Wasson *et al.* 2013), the marsh–upland ecotone appears to be migrating while plant community structure within the ecotone remains stable. This dynamic could be playing out across our monitoring sites, where new species appear to be moving into meadows and tidal flats from upland areas (Figure 8, Figure 11).

The changes in species cover and composition that we documented between 2007–2008 and 2018, while not enough points in time to establish a trend, are largely consistent with changes reported over the last half-century by Jorgenson et al. (2010). Our results suggest that coastal meadows and marshes have been largely stable in the last decade but may be showing changes in localized areas, and that the changes are pronounced and rapid, where they are occurring.

Initial Sampling in Coastal Meadows of Kenai Fjords National Park

Unlike salt marsh sites in LACL and KATM, the coastal marsh and meadow sites in KEFJ were sampled for the first time in 2018. Accordingly, the vegetation data we collected in KEFJ are primarily useful for site description until further sampling visits take place. That said, our sampling in 2018 revealed that the sites in KEFJ are dynamic systems that can host rapid vegetation development.

Coastal marshes at Long Beach, North Arm, and Beauty Bay in KEFJ stand apart from the salt marshes of LACL and KATM in multiple ways. The coastal marshes of KEFJ are considerably smaller in area than the three salt marsh systems that we monitor in the other two parks. Beauty Bay and North Arm are deltaic systems located in a protected fjord, in contrast to the barrier beach/lagoon geomorphology of Hallo Bay, Silver Salmon Creek, and Chinitna Bay. Long Beach conforms more closely to a barrier beach lagoon morphology. Whereas the 9.2 magnitude earthquake of 1964 uplifted the Cook Inlet coastline, the coastline of KEFJ subsided by 1.0–2.5 m (Lanik et al. 2018). This subsidence would have fully submerged any existing coastal marshes in Kenai Fjords, meaning that extant marshes were less than 55 years old at the time of our sampling.

Species composition at the KEFJ monitoring plots overlapped with that of the meadow systems in the other two parks and was most similar to species composition to the beach ridge geomorphic type in LACL and KATM (Figure 13). *Leymus mollis, Festuca rubra*, and *Lathyrus japonicus* were the

among the most abundant, ubiquitous and dominant species at all three sites in KEFJ (Table 4), and frequently co-occurred in plots. *Carex lyngbyei* was not among the most abundant or ubiquitous species but was locally dominant in a few plots (Table 5). *Potentilla anserina* subsp. *pacifica* was relatively common at Long Beach and North Arm where it co-occurred with *Leymus mollis* and *Festuca rubra*, but was rare in Beauty Bay (Table 4).

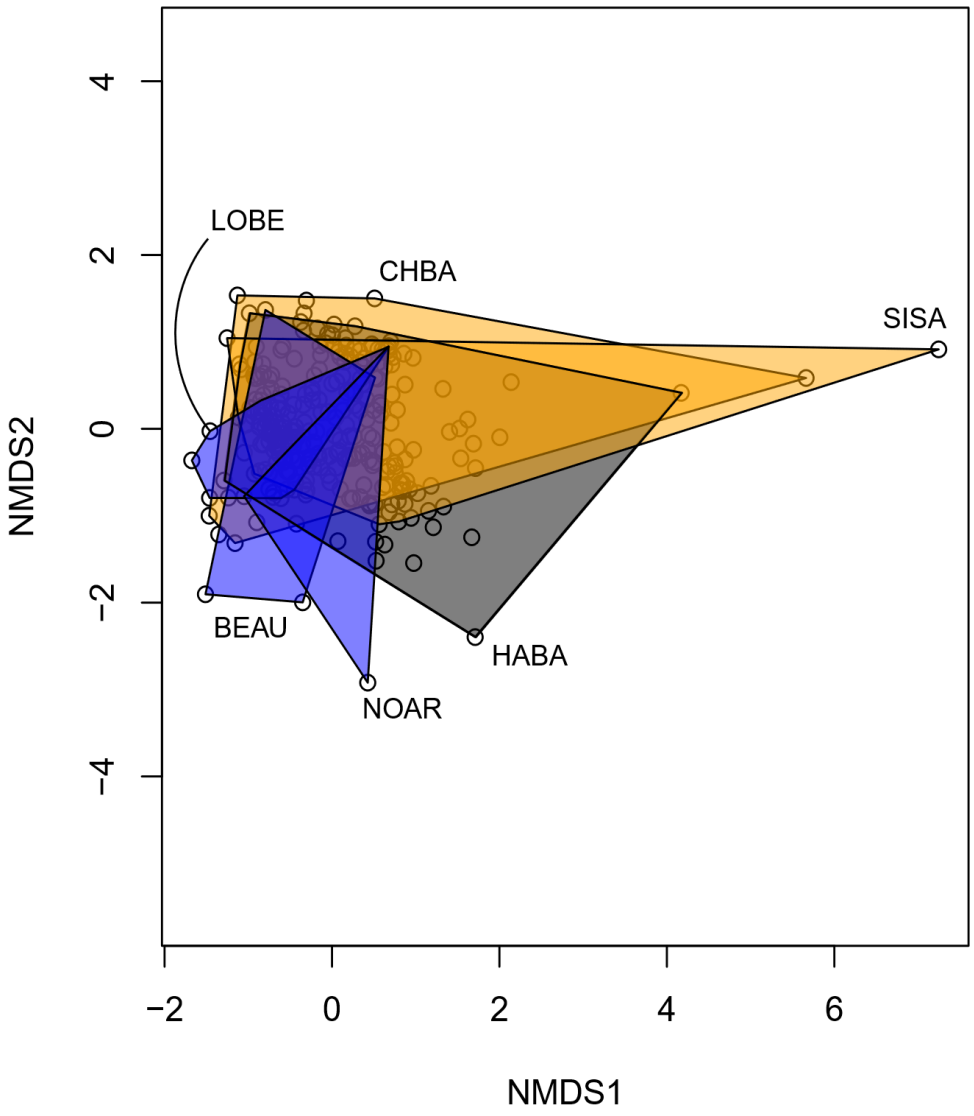

Figure 2. Vegetation composition of Kenai Fjords monitoring sites (Long Beach (LOBE), Beauty Bay (BEAU), North Arm (NOAR) differs from to those of Hallo Bay (HABA), Chinitna Bay (CHBA), and Silver Salmon Creek (SISA), and more closely resembles beach ridge communities than tidal flat communities. Top panel: convex hulls enclose all monitoring plots for each site in KEFJ (blue), KATM (grey), and LACL (amber).

Table 2. Mean and max cover, and frequency of occurrence at the plot-level of each species in Beauty Bay (BEAU, n=14), Long Beach (LOBE, n = 19), and North Arm (NOAR, n = 9) in Kenai Fjords National Park.

	Mean Cover			Max Cover			Frequency		
Species Name	**BEAU**	**LOBE**	**NOAR**	**BEAU**	**LOBE**	**NOAR**	**BEAU**	**LOBE**	**NOAR**
Leymus mollis subsp. *mollis*	0.210	0.448	0.398	1.000	1.000	1.000	0.500	0.895	0.667
Festuca rubra	0.134	0.240	0.184	0.720	1.000	0.760	0.571	0.526	0.444
Lathyrus japonicus	0.103	0.197	0.031	0.580	0.720	0.240	0.571	0.474	0.222
Poa eminens	0.083	0.001	0.027	0.900	0.020	0.240	0.214	0.053	0.111
Carex lyngbyei	0.081	0.075	0.220	0.720	0.940	1.000	0.214	0.211	0.222
Honckenya peploides	0.073	0.001	0.007	0.480	0.020	0.060	0.571	0.053	0.111
Rubus arcticus	0.047	0.000	0.000	0.660	0.000	0.000	0.071	0.000	0.000
Calamagrostis canadensis	0.040	0.025	0.000	0.260	0.380	0.000	0.214	0.105	0.000
Puccinellia nutkaensis	0.036	0.005	0.002	0.220	0.100	0.020	0.286	0.053	0.111
Galium aparine	0.027	0.000	0.000	0.340	0.000	0.000	0.143	0.000	0.000
Hierochloe odorata	0.021	0.000	0.000	0.300	0.000	0.000	0.071	0.000	0.000
Alnus viridis subsp. *sinuata*	0.010	0.018	0.000	0.140	0.280	0.000	0.071	0.105	0.000
Senecio pseudoarnica	0.007	0.000	0.000	0.100	0.000	0.000	0.071	0.000	0.000
Rhinanthus minor subsp. *groenlandicus*	0.006	0.000	0.000	0.080	0.000	0.000	0.071	0.000	0.000
Sanguisorba stipulata	0.006	0.000	0.000	0.060	0.000	0.000	0.143	0.000	0.000
Carex macrochaeta	0.004	0.000	0.000	0.060	0.000	0.000	0.071	0.000	0.000
Chamerion angustifolium	0.004	0.000	0.000	0.060	0.000	0.000	0.071	0.000	0.000
Polemonium acutiflorum	0.004	0.001	0.000	0.060	0.020	0.000	0.071	0.053	0.000
Achillea millefolium	0.003	0.032	0.000	0.040	0.480	0.000	0.071	0.211	0.000
Plantago maritima	0.003	0.000	0.000	0.020	0.000	0.000	0.143	0.000	0.000
Salix barclayi	0.003	0.000	0.000	0.040	0.000	0.000	0.071	0.000	0.000

Table 4 (continued). Mean and max cover, and frequency of occurrence at the plot-level of each species in Beauty Bay (BEAU, n=14), Long Beach (LOBE, n = 19), and North Arm (NOAR, n = 9) in Kenai Fjords National Park.

	Mean Cover			Max Cover			Frequency		
Species Name	**BEAU**	**LOBE**	**NOAR**	**BEAU**	**LOBE**	**NOAR**	**BEAU**	**LOBE**	**NOAR**
Heracleum maximum	0.001	0.000	0.000	0.020	0.000	0.000	0.071	0.000	0.000
Hordeum brachyantherum	0.001	0.000	0.004	0.020	0.000	0.040	0.071	0.000	0.111
Lysimachia maritima	0.001	0.002	0.000	0.020	0.040	0.000	0.071	0.053	0.000
Mertensia maritima var. *maritima*	0.001	0.000	0.000	0.020	0.000	0.000	0.071	0.000	0.000
Potentilla anserina subsp. *pacifica*	0.001	0.062	0.064	0.020	0.480	0.580	0.071	0.316	0.111
Rumex occidentalis S. Watson	0.001	0.000	0.000	0.020	0.000	0.000	0.071	0.000	0.000
Triglochin palustris	0.001	0.000	0.000	0.020	0.000	0.000	0.071	0.000	0.000
Picea sitchensis	0.000	0.027	0.000	0.000	0.320	0.000	0.000	0.105	0.000
Deschampsia cespitosa subsp. *beringensis*	0.000	0.020	0.000	0.000	0.300	0.000	0.000	0.158	0.000
Angelica lucida	0.000	0.013	0.000	0.000	0.240	0.000	0.000	0.053	0.000
Carex gmelinii	0.000	0.005	0.000	0.000	0.060	0.000	0.000	0.105	0.000
Atriplex gmelini	0.000	0.004	0.000	0.000	0.060	0.000	0.000	0.105	0.000
Cornus suecica	0.000	0.004	0.000	0.000	0.080	0.000	0.000	0.053	0.000
Trientalis europaea	0.000	0.004	0.002	0.000	0.080	0.020	0.000	0.053	0.111
Galium trifidum subsp. *trifidum*	0.000	0.003	0.042	0.000	0.060	0.220	0.000	0.053	0.222
Stellaria calycantha	0.000	0.003	0.000	0.000	0.040	0.000	0.000	0.105	0.000
Menziesia ferruginea	0.000	0.001	0.000	0.000	0.020	0.000	0.000	0.053	0.000
Poa sp.	0.000	0.001	0.000	0.000	0.020	0.000	0.000	0.053	0.000

Table 3. Floristic classes of each plot in KEFJ, based on predictions from random forest model trained on LACL and KATM vegetation data, and community types as determined by DeVelice et al. (1999). Pv is the proportion of models in the random forest ensemble that comprise the plurality for the predicted floristic class. A higher Pv suggests greater confidence in the chosen class.

Plot ID	Site	*RF-assigned Floristic Class*	Pv	Chugach NF Type (DeVelice et al. 1999)
BEAU-T1-100-S	BEAU	*Lathyrus maritimus-Senecio pseudoarnica*	0.46	Beach Pea
BEAU-T1-200-S	BEAU	Barren Beach	0.64	Seaside Sandplant
BEAU-T1-30-S	BEAU	*Lathyrus maritimus-Senecio pseudoarnica*	0.66	Beach Rye*†
BEAU-T1-300-S	BEAU	Barren Beach	0.40	Seaside Sandplant
BEAU-T2-200-S	BEAU	Barren Beach	0.12	Unclassified
BEAU-T2-300-S	BEAU	*Lathyrus maritimus-Senecio pseudoarnica*	0.68	Beach Rye*
BEAU-T2-400-S	BEAU	Barren Beach	0.42	Seaside Sandplant
BEAU-T2-500-S	BEAU	Barren Beach	0.58	Seaside Sandplant
BEAU-T2-600-W	BEAU	Barren Beach	0.54	Seaside Sandplant
BEAU-T2-700-W	BEAU	Barren Beach	0.36	Dwarf Alkaligrass
BEAU-T3-100-W	BEAU	Estuarine Water	0.22	Beach Rye*
BEAU-T3-200-W	BEAU	*Calamagrostis canadensis-Lupinus nootkatensis*	0.42	Bluejoint Reedgrass
BEAU-T4-300-W	BEAU	*Carex lyngbyaei-Cicuta virosa*	0.86	Lyngbye's sedge
BEAU-T4-400-W	BEAU	*Carex lyngbyaei-Cicuta virosa*	0.74	Lyngbye's sedge
LOBE-T1-1200-W	LOBE	Estuarine Water	0.32	Beach Rye*
LOBE-T1-1300-W	LOBE	*Lathyrus maritimus-Senecio pseudoarnica*	0.16	Beach Rye*
LOBE-T1-1400-W	LOBE	Estuarine Water	0.34	Beach Rye*
LOBE-T1-1500-W	LOBE	*Lathyrus maritimus-Senecio pseudoarnica*	0.44	Beach Rye*
LOBE-T1-1600-W	LOBE	*Lathyrus maritimus-Senecio pseudoarnica*	0.68	Beach Rye*
LOBE-T1-1700-W	LOBE	Estuarine Water	0.34	Beach Rye/Yarrow

* Beach Rye unless bryophytes = at least 15% cover; then Beach Rye/Yarrow

† *Festuca rubra* represents most dominant species.

Table 5 (continued). Floristic classes of each plot in KEFJ, based on predictions from random forest model trained on LACL and KATM vegetation data, and community types as determined by DeVelice et al. (1999). Pv is the proportion of models in the random forest ensemble that comprise the plurality for the predicted floristic class. A higher Pv suggests greater confidence in the chosen class.

Plot ID	Site	*RF-assigned Floristic Class*	Pv	Chugach NF Type (DeVelice et al. 1999)
LOBE-T2-100-W	LOBE	*Carex lyngbyaei-Cicuta virosa*	0.46	Beach Rye*
LOBE-T2-1000-W	LOBE	*Lathyrus maritimus-Senecio pseudoarnica*	0.30	Beach pea
LOBE-T2-1100-W	LOBE	Estuarine Water	0.16	Beach pea
LOBE-T2-1200-W	LOBE	*Lathyrus maritimus-Senecio pseudoarnica*	0.40	Beach pea
LOBE-T2-200-W	LOBE	*Elymus mollis-Plantago maritima*	0.24	Beach Rye*†
LOBE-T2-300-W	LOBE	*Elymus mollis-Plantago maritima*	0.24	Beach Rye*
LOBE-T2-400-W	LOBE	*Elymus mollis-Plantago maritima*	0.20	Beach Rye*
LOBE-T2-500-W	LOBE	*Elymus mollis-Plantago maritima*	0.24	Beach Rye*
LOBE-T2-600-W	LOBE	*Lathyrus maritimus-Senecio pseudoarnica*	0.20	Beach Rye*
LOBE-T2-800-W	LOBE	*Carex lyngbyaei-Cicuta virosa*	0.92	Lyngbye's sedge
LOBE-T2-900-W	LOBE	*Lathyrus maritimus-Senecio pseudoarnica*	0.72	Beach Rye*
LOBE-T3-300-W	LOBE	*Lathyrus maritimus-Senecio pseudoarnica*	0.68	Beach Rye*†
LOBE-T3-700-W	LOBE	*Lathyrus maritimus-Senecio pseudoarnica*	0.62	Beach pea
NOAR-T1-100-W	NOAR	*Elymus mollis-Plantago maritima*	0.22	Beach Rye*
NOAR-T1-200-W	NOAR	Estuarine Water	0.22	Beach Rye*
NOAR-T2-100-W	NOAR	*Carex lyngbyaei-Cicuta virosa*	0.74	Lyngbye's sedge
NOAR-T2-150-W	NOAR	*Carex lyngbyaei-Cicuta virosa*	0.92	Lyngbye's sedge
NOAR-T2-60-W	NOAR	*Lathyrus maritimus-Senecio pseudoarnica*	0.18	Beach Rye*
NOAR-T3-0-W	NOAR	*Achillea millefolium-Carex gmelinii*	0.20	Beach Rye*
NOAR-T3-50-W	NOAR	Barren Beach	0.66	Beach Rye*
NOAR-T4-100-W	NOAR	Estuarine Water	0.22	Beach Rye*
NOAR-T4-150-W	NOAR	Estuarine Water	0.30	Dwarf Alkaligrass

* Beach Rye unless bryophytes = at least 15% cover; then Beach Rye/Yarrow

† *Festuca rubra* represents most dominant species.

We applied the random forest trained on 2007–2008 data from LACL and KATM to classify plots sampled in KEFJ, but the results mostly revealed that KEFJ plant communities differ from those at KATM and LACL. The most common floristic class sampled in KEFJ's coastal meadows was classified as *Lathyrus maritimus-Senecio pseudoarnica* (13 plots). However, only one of these plots contained *Senecio pseudoarnica*. Likewise, the *Carex lyngbyaei-Cicuta virosa* floristic class was identified at all three sites in KEFJ (6 plots) despite the absence of *Cicuta virosa*. Plant community types described from the Chugach National Forest/Prince William Sound (DeVelice et al. 1999) may be more applicable to KEFJ vegetation. Classifying KEFJ plots according to this scheme yielded mostly plots belonging to the Beach Rye (26 plots), Beach Pea (5 plots), and Seaside Sandplant community types (5 plots; Table 4). Many of our plots had substantial cover of *Festuca rubra*, which was rarely mentioned in the classification scheme of DeVelice et al. (1999).

Although we couldn't assess vegetation change based on a single sampling event, we encountered evidence of rapid landscape change and vegetation response. Satellite and aerial photos of Beauty Bay from 2005 and 2016 show substantial vegetation colonization of gravel bars (Figure 14). Plot sampling at this site revealed the potential for rapid vegetation colonization and growth. Several plots at this site featured *Honckeyna peploides* and *Puccinellia nuttallii* colonizing bare sand, and another plot, further inland, featured thick growth of grass and Sitka alder (*Alnus viridis* subsp. *sinuata*) that appeared to have established since 2005 (Figure 14).

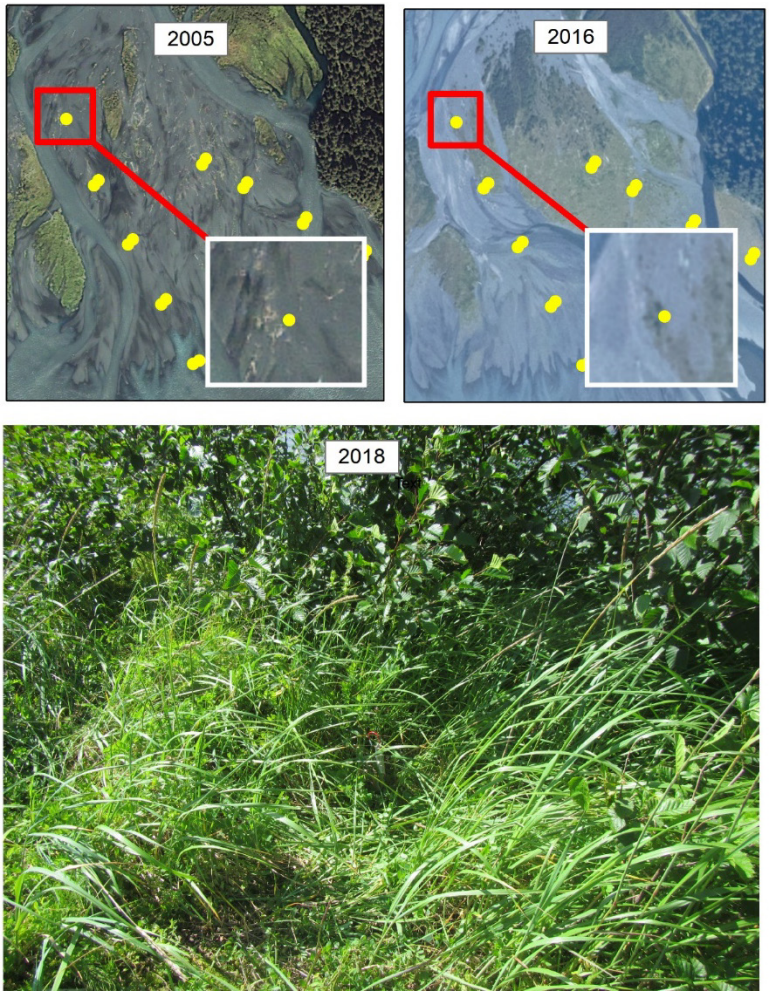

Figure 14. Evidence of rapid colonization of gravel bars following channel migration at Beauty Bay. The top two panels show an overview of transects, with an enlarged (white box) view of the area surrounding one plot (red box). Satellite imagery in 2005 suggest little to no vegetation, and aerial photography collected in 2016 and a plot photograph from 2018 show dense alder and grass cover.

Literature Cited

Anderson, M. J. 2001. A new method for non-parametric multivariate analysis of variance. Austral Ecology 26(1):32–46. doi:10.1046/j.1442-9993.2001.01070.x

Anderson, M. J. 2017. Permutational Multivariate Analysis of Variance (PERMANOVA). Wiley StatsRef: Statistics Reference Online:1–15. doi:10.1002/9781118445112.stat07841

Bennet, A. J. 1996. Physical and biological resource inventory of the Lake Clark National Park-Cook Inlet Coastline, 1994–1996. Kenai, Alaska.

Conn, P. B., D. S. Johnson, P. J. Williams, S. R. Melin, and M. B. Hooten. 2018. A guide to Bayesian model checking for ecologists. Ecological Monographs 88(4):526–542. doi:10.1002/ecm.1314

Cusick, J., and A. J. Bennet. 2005. Morphological shoreline changes along the Lake Clark National Park-Cook Inlet coast, 1992–1994. Anchorage, Alaska.

DeVelice, R. L., C. J. Hubbard, K. Boggs, S. Boudreau, M. Potkin, T. Boucher, and C. Wertheim. 1999. Plant community types of the Chugach National Forest: Southcentral Alaska. Anchorage, Alaska.

Fraser, R. H., T. C. Lantz, I. Olthof, S. V. Kokelj, and R. A. Sims. 2014. Warming-induced shrub expansion and lichen decline in the Western Canadian Arctic. Ecosystems 17(7):1151–1168. doi:10.1007/sl0021-014-9783-3

Freymueller, J. T., H. Woodard, S. C. Cohen, R. Cross, J. Elliott, C. F. Larsen, S. Hreinsdóttir, and C. Zweck. 2013. Active deformation processes in Alaska, based on 15 years of GPS measurements. Active Tectonics and Seismic Potential of Alaska:1–42. doi:10.1029/179GM02

Gelman, A. 2006. Prior distributions for variance parameters in hierarchical models (comment on article by Browne and Draper). Bayesian Analysis 1(3):515–534. doi:10.1214/06-BA117A

Gelman, A. 2008. Scaling regression inputs by dividing by two standard deviations. Statistics in Medicine 27(15):2865–2873. doi:10.1002/sim

Gelman, A., A. Jakulin, M. G. Pittau, and Y. S. Su. 2008. A weakly informative default prior distribution for logistic and other regression models. Annals of Applied Statistics 2(4):1360–1383. doi:10.1214/08-AOAS191

Gelman, A., and D. B. Rubin. 1992. Inference from iterative simulation using multiple sequences. Statistical Science 7(4):457–511. doi:10.2307/2246134

Gill, Jr., R. E., and T. L. Tibbitts. 1999. Seasonal shorebird use of intertidal habitats of Cook Inlet, Alaska. Vol. MMS 99–001. Seattle, Washington.

Hill, G. B, and G. H. R. Henry. 2011. Responses of high arctic wet sedge tundra to climate warming since 1980. Global Change Biology 17(1):276–287. doi:10.1111/j.1365-2486.2010.02244.x

Jorgenson, M. T., G. V. Frost, W. E. Lentz, and A. J. Bennet. 2006. Photographic monitoring of landscape change in the Southwest Alaska Network of national parklands, 2006. Fairbanks, Alaska.

Jorgenson, M T., J. E. Roth, S. F. Schlentner, E. R. Pullman, M. Macander, and C. H. Racine. 2003. An ecological land survey for Fort Wainwright, Alaska. Hanover, New Hampshire.

Jorgenson, T., G. V. Frost, A. E. Miller, P. Spencer, M. Shephard, B. A. Mangipane, C. Moore, and C. Lindsay. 2010. Monitoring coastal salt marshes in the Lake Clark and Katmai National Parklands of the Southwest Alaska Network. Natural Resource Technical Report. NPS/SWAN/NRTR—2010/338. National Park Service, Fort Collins, Colorado.

Jorgenson, T. M., G. V. Frost, and D. Dissing. 2018. Drivers of landscape changes in coastal ecosystems on the Yukon-Kuskokwim Delta, Alaska. Remote Sensing 10(8):1–27. doi:10.3390/rs10081280

Jorgenson, T. M., and A. E. Miller. 2010. Protocol for monitoring coastal salt marshes in the Southwest Alaska Network. Natural Resource Report. NPS/SWAN/NRR—2009/154. National Park Service, Fort Collins, Colorado.

Kellner, K. 2018. jagsUI: A wrapper around “rjags” to streamline “JAGS” analyses.

Kennish, M. J. 2002. Environmental threats and environmental future of estuaries. Environmental Conservation 29(1):78–107. doi:10.1017/S0376892902000061

Kirwan, M. L., and L. K. Blum. 2011. Enhanced decomposition offsets enhanced productivity and soil carbon accumulation in coastal wetlands responding to climate change. Biogeosciences 8(4):987–993. doi:10.5194/bg-8-987-2011

Kirwan, M. L., and J. P. Megonigal. 2013. Tidal wetland stability in the face of human impacts and sea-level rise. Nature 504(7478):53–60. doi:10.1038/nature12856

Lanik, A., C. P. Hults, and D. Kurtz. 2018. Kenai Fjords National Park: Geologic Resources Inventory Report. Fort Collins, Colorado.

Miller, A. E., W. L. Thompson, C. Mortenson, and C. Moore. 2010. Protocol for ground-based monitoring of vegetation in the Southwest Alaska Network.

Morris, J. T., P. V. Sundareshwar, C. T. Nietch, B. Kjerfve, and D. R. Cahoon. 2002. Responses of coastal wetlands to rising sea level. Ecology 83(10):2869–2877. doi:10.1890/0012-9658(2002)083[2869:ROCWTR]2.0.CO;2

Oksanen, J., F. G. B.lanchet, M. Friendly, R. Kindt, P. Legandre, D. McGlinn, P. R. Minchin, R. B. O'Hara, G. L. Simpson, P. Solymos, M. H. H. Stevens, E. Szoecs, and H. Wagner. 2019. Vegan: an introduction to ordination. Vegan: Community Ecology Package.

Peters, D. P. C., J. R. Gosz, T. Pockman, E. E. Small, R. R. Parmenter, S. L. Collins, and E. Muldavin. 2006. Integrating patch and boundary dynamics to understand and predict biotic transitions at multiple scales. Landscape Ecology 21(1):19–33. doi:10.1007/s10980-005-1063-3

Plummer, M. 2017. JAGS Version 4.3.0 user manual.

R Core Team. 2019. R: A language and environment for statistical computing. R Foundation for Statistical Computing, Vienna, Austria.

Redfield, A. C. 1965. Ontogeny of a salt marsh estuary. Science 147(3653):50–55. doi:10.1210/jcem-10-10-1361

Redfield, A. C. 1972. Development of a New England salt marsh. Ecological Monographs 42(2):201–237. doi:10.1063/1.4900737

Rode, K. D., C. T. Robbins, and L. A. Shipley. 2001. Constraints on herbivory by grizzly bears. Oecologia 128(1):62–71. doi:10.1007/s004420100637

Shugar, D. H., I. J. Walker, O. B. Lian, J. B. R. Eamer, C. Neudorf, D. McLaren, and D. Fedje. 2014. Post-glacial sea-level change along the Pacific coast of North America. Quaternary Science Reviews 97:170–192. doi:10.1016/j.quascirev.2014.05.022

Smith, T. S., and S. T. Partridge. 2004. Dynamics of intertidal foraging by coastal brown bears in Southwestern Alaska. Journal of Wildlife Management 68(2):233–240. doi:10.2193/0022-541x(2004)068[0233:doifbc]2.0.co;2

Ulman, S. E. G., C. K. Williams, J. M. Morton, T. L. DeLiberty, and B. N. Ness. 2019. Vegetation change on an Alaska estuary after the 1964 great Alaska earthquake. Northwest Science 93(1):16. doi:10.3955/046.093.0103

Villarreal, S., R. D. Hollister, D. R. Johnson, M. J. Lara, P. J. Webber, and C. E. Tweedie. 2012. Tundra vegetation change near Barrow, Alaska (1972–2010). Environmental Research Letters 7(1). doi:10.1088/1748-9326/7/1/015508

Wasson, K., A. Woolfolk, and C. Fresquez. 2013. Ecotones as indicators of changing environmental conditions: Rapid migration of salt marsh-upland boundaries. Estuaries and Coasts 36(3):654–664. doi:10.1007/s12237-013-9601-8

Appendix A: Sample Sufficiency

Power Analysis

We performed a simulation to understand our power to detect change in vegetation cover, and how our sampling scheme affected that power. Of particular interest was the effect of varying within plot sample size and the number of plots sampled. We used single-species data for *Carex lyngbyei*, as detecting change in common species was our primary goal.

We used a two-step approach. First, while fitting a Bayesian regression model to estimate the cover of a single species from 2007–2008 data, we simulated new plot data (number of hits for a species) using the parameters being estimated and a fixed value to represent a hypothetical increase in cover on the log-odds scale. We created 500 simulated data sets in this manner, that would represent cover at the initial and second sampling event. Second, we used the same model to analyze the simulated data, estimating species cover and the difference in cover between years for each of these 500 simulated datasets. We could then examine how often out of the 500 simulations we detected an increase in cover at multiple levels of certainty.

Our regression model is a hierarchical logistic regression with random effects for plot-level intercepts and slopes.

We envision a two-level process, where each site i has some probability of hosting the focal species. H_i is the binary factor representing whether or not plot i is suitable habitat for the focal species:

$$H_{i,1} \sim \text{Bernoulli}(f_1)$$

where f_1 is the plot-level frequency of occurrence of the suitable habitat for focal species at time 1.

At suitable plots, the focal species may occur at different densities. Our point intercept sampling yields a discrete number of 'hits' (y), governed by the proportional cover of that species. So the number of hits at site i and time 1 is:

$$y_{i,1} \sim \text{binomial}(\psi_{i,1} \cdot P_{i,1}, 100)$$

Where $P_{i,1}$ is the proportional cover of the focal species in plot i, at time one. We model the proportional cover at plot i, P_i using a logit link function, as

$$\frac{P_{i,1}}{1 + P_{i,1}} = \alpha_i$$

where α_i corresponds to the log-odds of presence of the focal species within plot i, and is drawn from a normal distribution whose parameters represent the population level average μ and standard deviation σ of the log odds of presence of the focal species.

$$\alpha_i \sim N(\mu, \sigma)$$

This distribution is, in turn used to generate our simulated data, in the same model. After burn-in of the Markov chain monte carlo (MCMC) sampler, we generate one full simulated data set for each MCMC iteration.

Then our simulated number of point intercept 'hits' for our focal species at plot i at time t and MCMC iteration k is:

$$z_{i,t,k} \sim \text{binomial}(\psi_{i,t,k} \cdot P_{i,t,k}, n_i)$$

where $p_{i,t,k}$ is the proportional cover at plot i, time t, and MCMC iteration k, and n_i is the number of points sampled. We model the proportional cover at each plot using a logit link function, as

$$log(\frac{P_{i,t,k}}{1+P_{i,t,k}}) = \alpha_{i,k}{}' + \delta_{i,t,k}$$

where _{i,t,k} represents change in cover on the log-odds scale, and is set to 0 at time 1 and a chosen change amount at time two. drawn from a normal distribution at time 2:

$$\delta_{i,2,k} \sim N(u, \varsigma)$$

We supply the population average change in time u, and the standard deviation of change, ς, chosen to represent expected rates of change in species cover.

Each simulated plots starting cover, $\alpha_i{}'$ is drawn from a normal distribution with the population parameters estimated in the models fit to the data at that MCMC iteration.

$$\alpha_{i,k}{}' \sim N(\mu_k, \sigma_k)$$

Written in the JAGS language, here is our simulation-generating model

```
{
sink(file = "Sing_spc_mod1.r")#U:/Research/Salt_marsh_explore/Sing_Spc_mod1.r
")
 cat(
"
model{
 for(i in 1:N_plots){
  y[i]   ~ dbinom(psi[i] * p[i], n_points[i])
  psi[i]  ~ dbern(f)
  #p[i]  ~ dbeta(alpha,beta)
  p[i]  <- ilogit(alpha[i])
  alpha[i] ~ dnorm(mu, tau)

  #Post predictive checks
  y_pred[i] ~ dbinom(psi[i] *p[i], n_points[i])

 }
 # pp.mean <- step(mean(y) - mean(y_pred))
 # pp.sd  <- step(sd(y) - sd(y_pred))
 # pp.y  <- mean(step(y_pred[] - y[]))
```

```
 f <-1 #~ dbeta(1,1)
 # alpha <- 1
 # beta <- 1

 mu ~ dnorm(0, .3)
 tau ~ dnorm(0,.25)T(0,) #<- sd_p^-2
 #sd_p ~ dunif(0,100)


 # Simulate new observations
 for(i in 1:N_plots){
  for(t in 1:2){
   y_new[i,t]  ~ dbinom(psi_new[i,t] * p_new[i,t], n_points_new)
   psi_new[i,t] <- psi[i]  #dbern(psi[i] * p_pers + (1-psi[i]) * p_col)
   p_new[i,t]  <- ilogit(alpha[i] + alpha_chg[i,t])
   #p_change[i] ~ dgamma(prop_change^2/prop_chg_SD^2, prop_change/prop_chg_SD
^2)
  }
  alpha_chg[i,1] <- 0
  alpha_chg[i,2] ~ dnorm(delta, sigma^-2)
 }
 #f_new <- f * f_change
 delta <- change_log_odds
 sigma <- chg_log_odds_SD
 #
 # #Derived quantities
 # # p_av <- alpha/(alpha+beta)
 # # p_sig <- alpha*beta/((alpha + beta)^2 * (alpha + beta + 1))
 # # p_draw ~ dbeta(alpha,beta)
  }
", fill = TRUE)
sink()
}
```

Below, we prepare data for the simulation-generating model:

```
library(dplyr)
library(ggplot2)
library(tidyr)

# Marsh_Pt_Int <- read.csv("U:\\Research\\Salt_marsh_explore\\Salt Marsh Data
- Species_Observations.csv",
#             skip = 2, as.is = c(2,3),
#             header = TRUE)
Marsh_Pt_Int <- read.csv("../../Salt Marsh Data - Species_Observations.csv",
             skip = 2, as.is = c(2,3),
             header = TRUE)
Marsh_Pt_Int$Species_Code2 <- factor(tolower(Marsh_Pt_Int$Species_Code))
Marsh_Pt_Int$SpeciesName  <- factor(tolower(Marsh_Pt_Int$SpeciesName))
Marsh_Pt_Int$Species_Code <- Marsh_Pt_Int$Species_Code2

n_points_new = 50
n_plots_added = 100

Pt_Int_Wide = select(Marsh_Pt_Int, CountOfSpeciesName, Species_Code2, SiteID)
%>%
```

```
 spread(Species_Code2, CountOfSpeciesName, fill = 0)
Pt_Int_Wide$n = rowSums(Pt_Int_Wide[,-1])
Pt_Int_Wide = filter(Pt_Int_Wide, n>10)



new_plots = matrix(nrow = n_plots_added, ncol = dim(Pt_Int_Wide)[2])
new_plots_df = as.data.frame(new_plots)
names(new_plots_df) = names(Pt_Int_Wide)
new_plots_df$n = 100

Pt_Int_Wide = rbind(Pt_Int_Wide, new_plots_df)
# add rows of NA to Pt_Int_Wide to simulate more plots

my_dat <- list(
 y = Pt_Int_Wide$carlyn,
 n_points = Pt_Int_Wide$n,
 N_plots = dim(Pt_Int_Wide)[1],
 n_points_new = n_points_new,
 f_change = 1,
 change_log_odds = .4,
 chg_log_odds_SD = .4
)
```

Below is a little exploration of our change function for percent cover. The approach is just to add a constant to the log odds of presence, in other words add a constant to the intercept of our logistic regression function. This constrains the change to be on the unit scale, and results in smaller increases for higher covers and smaller decreases for lower covers, generally speaking. We make some graphics to help build intuition about this change function, and to pick reasonable change values on the log-odds scale. A reasonably close match to change amount used by the power analysis in (Jorgenson et al. 2010) corresponds to an increase of 0.4 on the log-odds scale. For our power analysis below, we'll use values of 0.1 and 0.4 (Figures A-1 to A-3), with standard deviations of 0.2, 0.4, and 0.8.

```
x = seq(-4,4,.1)
lx = exp(x)/(1+exp(x))
logit <- function(x,d){
 out.y <- exp(x+d)/(1+exp(x+d))
 df <- cbind(out.y, d)
 return(as.data.frame(df))
}

lx = logit(x,0)
y.5 = logit(x, .4)
y.1 = logit(x, .1)
y1.0 = logit(x, 1)
y2.0 = logit(x, 2)
yn.5 = logit(x, -.4)
yn.1 = logit(x, -.1)
yn1.0 = logit(x, -1)
yn2.0 = logit(x, -2)
df = rbind(lx, y.5, y.1, y1.0, y2.0, yn1.0, yn.5, yn.1, yn2.0)

df$x = rep(x,9)
```

```
df$lx = rep(lx$out.y,9)
df$dif = df$out.y-df$lx
df$d = factor(df$d)

ggplot(df, aes(x = lx, y = dif, group = d, colour = d) ) +
 geom_line() +
 theme_bw() +
 scale_y_continuous(breaks = seq(-.5,.5,.1)) +
 scale_x_continuous(breaks = seq(0,1,.1)) +
 ylab('Mean Change in proportional cover') + xlab('Mean starting proportional
cover')
```

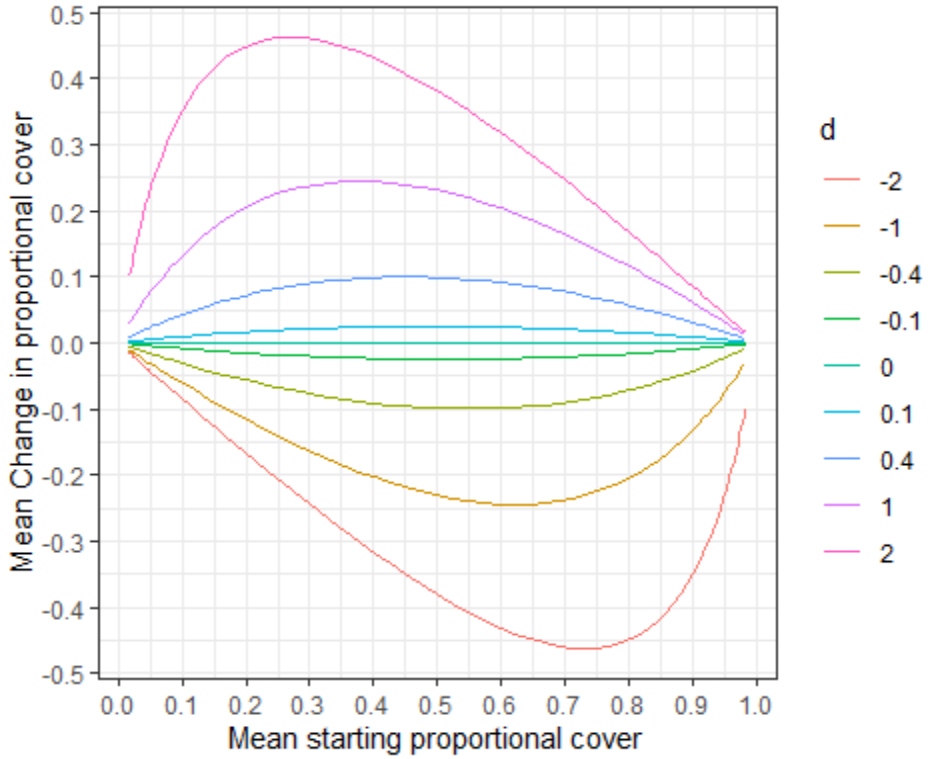

Figure A-1. Change in proportional cover as a function of starting proportional cover for different values of the change in log-odds of cover (d).

```
ggplot(df, aes(x = lx, y = out.y, group = d, colour = d) ) +
 geom_line() +
 theme_bw() + ylab('Mean ending proportional cover') + xlab('Starting proport
ional cover')
```

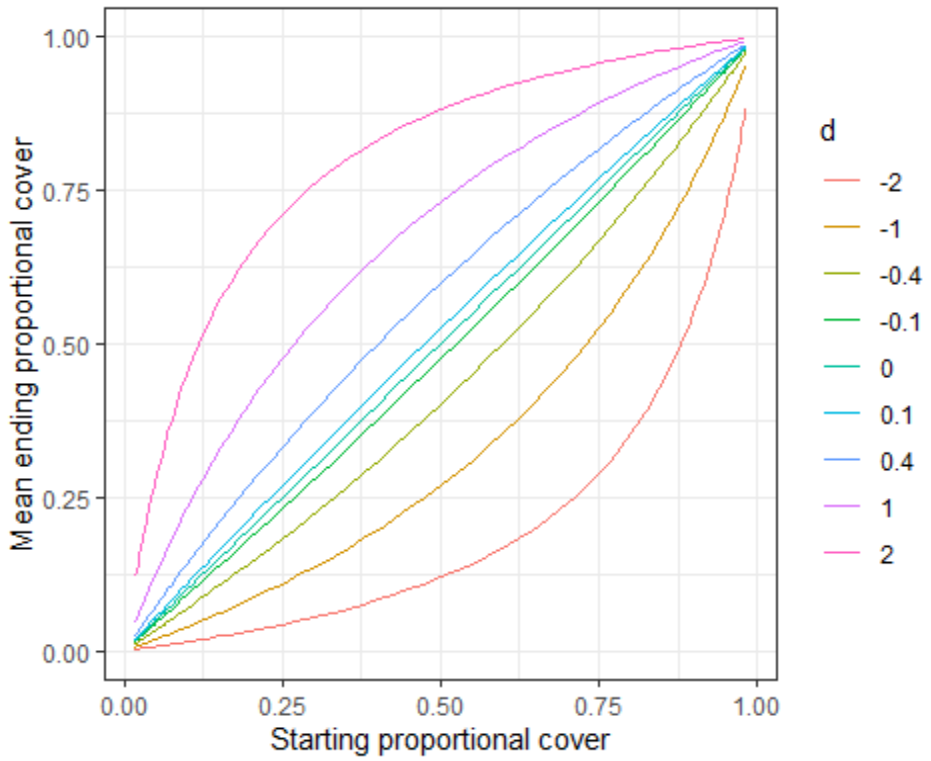

Figure A-2. Ending proportional cover as a function of starting proportional cover for different values of the change in log-odds of cover (d).

```
ggplot(df, aes(x = x, y = out.y, group = d, colour = d) ) +
 geom_line() +
 theme_bw() + ylab('Mean ending proportional cover') + xlab('Log odds of star
ting cover')
```

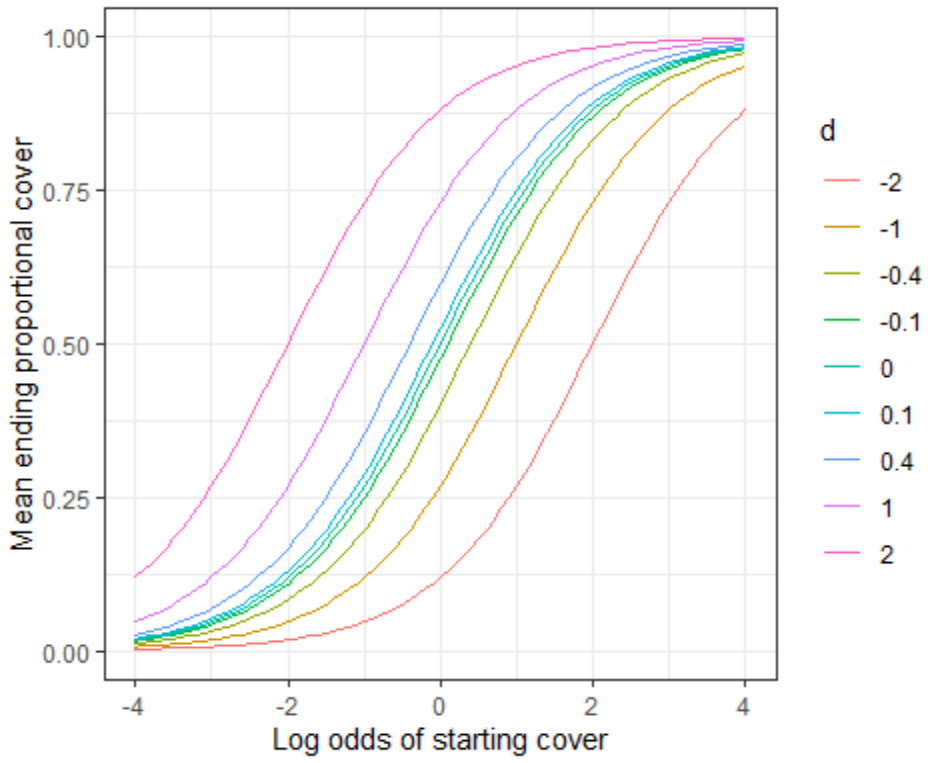

Figure A-3. Ending proportional cover as a function of starting log odds of cover for different values of the change in log-odds of cover (d).

```
{
sink("Sing_Spc_Power.r")#U:/Research/Salt_marsh_explore/Sing_Spc_Power.r")
cat("
model{
for(m in 1:n_Sims){
 for(i in 1:N_plots){
  for(t in 1:2){
   y_new[i,t,m] ~ dbinom(psi[i,t,m] * p[i,t,m], n_points_new)
   psi[i,t,m]  ~ dbern(f[m])
   p[i,t,m]   <- ilogit(alpha[i,m] + delta[i,t,m])
  }
  alpha[i,m] ~ dnorm(mu[m], tau[m])
  delta[i,2,m] ~ dnorm(u[m], taud[m])
  delta[i,1,m] <-0
  # p_new[i,m] <- ilogit(a_new[i,m])
  # a_new[i,m] ~ dnorm(u2[m], tau2[m])
 }
 f[m] <-1 #~ dbeta(1,1)
 u[m]  ~ dnorm(0, .3)  # ~ dt(0,.2, 4)
 mu[m] ~ dnorm(0, .3)
 tau[m] ~ dnorm(0,.25)T(0,)  #dt(0, .25, 3)T(0,) #sigma[m]^-2
 taud[m] ~ dnorm(0,.25)T(0,)

 # u2[m] ~ dnorm(0, .3)
 # tau2[m] ~ dnorm(0,.25)T(0,) #dt(0, .25, 3)T(0,)
}
}
```

```
", fill = TRUE)
sink()
}
```

Now we'll run our power analysis. Our input data has 500 simulations for each sample plot at times one and two given our selected rate of change. For each of these simulated data sets, we'll estimate the average proportional cover of CARLYN across all study plots at time one and the average change in cover between times, giving us 500 estimated changes in cover. These are estimated at each MCMC step giving us a posterior distribution of the estimated change in CARLYN for each of the simulated data sets. That gives us the Bayesian version of our p-value for each simulated data set. We then look across our 500 simulations, to see how many times we found a probability of increase (p) greater than α. Here, we use α to indicate a posterior probability. So, if we estimate a power of 0.80, at α=0.95, that would mean that 80% of the time, we would detect the correct direction of change with greater than 95% certainty.

```
n_points_new = 50
n_plots_added = 100
change_log_odds = .4
chg_log_odds_SD = .4

parameters <- data.frame(
 n_points_new = rep(rep(c(100, 50, 50), 3), 2),
 n_plots_added = rep(rep(c(0, 0, 50), 3), 2),
 change_log_odds = c(rep(.4, 9), rep(.1, 9)),
 ch_log_odds_SD = rep(c(rep(.2,3), rep(.4, 3), rep(.8, 3)),2)
)
power_out = as.data.frame(array(NA, dim = c(18,9)))
names(power_out) = c(names(parameters), 'Q.975','Q.9', 'Q.5', 'Q.1','Q.025')

for(i in 1:18){#1:dim(parameters)[1]){
 print(i)
 n_points_new  = parameters$n_points_new[i]
 n_plots_added  = parameters$n_plots_added[i]
 change_log_odds = parameters$change_log_odds[i]
 chg_log_odds_SD = parameters$ch_log_odds_SD[i]

 #format source data
 Pt_Int_Wide = select(Marsh_Pt_Int, CountOfSpeciesName, Species_Code2, SiteID
) %>%
  spread(Species_Code2, CountOfSpeciesName, fill = 0)
 Pt_Int_Wide$n = rowSums(Pt_Int_Wide[,-1])
 Pt_Int_Wide = filter(Pt_Int_Wide, n>10)


 #add 'new' plots
 if(n_plots_added>0){
  new_plots = matrix(nrow = n_plots_added, ncol = dim(Pt_Int_Wide)[2])
  new_plots_df = as.data.frame(new_plots)
  names(new_plots_df) = names(Pt_Int_Wide)
  new_plots_df$n = 100
  Pt_Int_Wide = rbind(Pt_Int_Wide, new_plots_df)
 }
```

```
 #compile data for simulation run
 my_dat <- list(
  y = Pt_Int_Wide$carlyn,
  n_points = Pt_Int_Wide$n,
  N_plots = dim(Pt_Int_Wide)[1],
  n_points_new = n_points_new,
  f_change = 1,
  change_log_odds = change_log_odds,
  chg_log_odds_SD = chg_log_odds_SD
 )

 carlyn.jags <- jags.model("Sing_Spc_mod1.r",
              data = my_dat, n.chains = 3)#,
 #inits = my.inits)

 update(carlyn.jags, 5000)
 carlyn.sim = jags.samples(carlyn.jags, n.iter = 500, variable.names = c('y_n
ew','mu', 'alpha'))

 sim_out <- carlyn.sim

 sim_dat <- list(
  y_new = sim_out$y_new[,,,1],
  #alpha = sim_out$alpha[,,1],
  n_Sims = dim(sim_out$y_new)[3],
  N_plots = dim(sim_out$y_new)[1],
  n_points_new = n_points_new,
  mu = sim_out$mu[1,,1]
 )

 pow.jags <- jags.model(file = "Sing_Spc_Power.r", n.chains = 3,
             data = sim_dat)#, inits = pow.inits)
 pow.jsamp = jags.samples(pow.jags, n.iter = 1000, variable.names = 'u') #c('
delta', 'u', 'p_new[1,1]'))

 power.sum <- summary(pow.jsamp$u, FUN = 'quantile', c(.975, .9, .5,.1,.025))
$stat

 power.vals = apply(power.sum, FUN = function(x){mean(x>0)}, MARGIN = 1)

 power_out[i,] <- as.vector(c(parameters[i,], power.vals))
}
```

Halving the within-plot point density while adding 50 plots led to better power to detect small changes (d =0.1, Figure A-1) in cover at α =0.08, and at α =0.95 except for the highest level of within plot variability in between-year change (Table A-1). This sampling scheme also led to similar power at larger magnitudes of between-year change (d=0.4, Figure A-1, Table A-1). Halving the within-plot point density without adding additional plots yielded the lowest power at all magnitudes of change and levels of among-plot variability in change magnitude, but still yielded power ≥ 0.80 for larger magnitudes of change at α=0.80.

Table A-1. Bayesian power simulation results for combinations of within plot point density (Points per plot, 2 levels), number of new plots added (Plots added, 2 levels), change between years (2 magnitudes), and among-plot standard deviation of change magnitude (3 magnitudes). Power from 500 simulations expressed as the proportion of estimates that detected the simulated increase in cover at various levels of certainty.

Points per plot	Plots added	Change log_odds	SD change log odds	Power*		
				α=0.5†	α=0.8†	α=0.95†
100	0	0.4	0.2	1.000	1.000	0.976
50	0	0.4	0.2	0.998	0.948	0.830
50	50	0.4	0.2	1.000	0.998	0.954
100	0	0.4	0.4	1.000	0.986	0.922
50	0	0.4	0.4	1.000	0.978	0.794
50	50	0.4	0.4	1.000	0.988	0.904
100	0	0.4	0.8	0.992	0.882	0.662
50	0	0.4	0.8	0.990	0.800	0.576
50	50	0.4	0.8	0.998	0.924	0.740
100	0	0.1	0.2	0.796	0.158	0.026
50	0	0.1	0.2	0.732	0.144	0.018
50	50	0.1	0.2	0.804	0.192	0.046
100	0	0.1	0.4	0.774	0.184	0.048
50	0	0.1	0.4	0.718	0.148	0.034
50	50	0.1	0.4	0.814	0.266	0.070
100	0	0.1	0.8	0.670	0.212	0.086
50	0	0.1	0.8	0.652	0.174	0.052
50	50	0.1	0.8	0.694	0.232	0.074

* Power is here defined as the proportion of estimates that detected the simulated increase at the given level of certainty.

† Here we define α as the proportion of the posterior density that is > 0, which indicates the estimated probability that the change in cover is >0

Post Sampling Review

During the 2018 vegetation plot revisits, we reduced the point intercept sampling intensity from 100 points per plot to 50 points per plot. To investigate whether 50 points per plot is adequate to capture the community composition in our 4 x 10m plots, we examined species accumulation curves for each plot, during each sampling visit.

Species accumulation curves summarize the number of species encountered in successively larger samples of the data. In our case, within each plot, our point intercept observations were permuted: randomly resampled without replacement. Graphic summaries for each sample plot display the mean number of species (+/− SD) found at a single point intercept, two points, three points, and so forth up to the maximum number of points sampled at that plot. Species accumulation curves are expected to rise steeply, and then level off as they approach the actual species richness at that plot. At steeper

portions of the curve, additional points measured are more likely to detect new species than at flatter portions of the curve. Therefore, if the species accumulation curve is still ascending steeply at the maximum number of sample points, that plot has likely not captured a substantial portion of the species present.

At the most species-rich plots, it appeared that neither the 50 point nor 100 point intensity was entirely sufficient. Generally, species were accumulated at the same rate in both sampling intervals, and it didn't appear that either sampling interval had consistently higher species richness. These results suggest caution when making inferences about rare species.

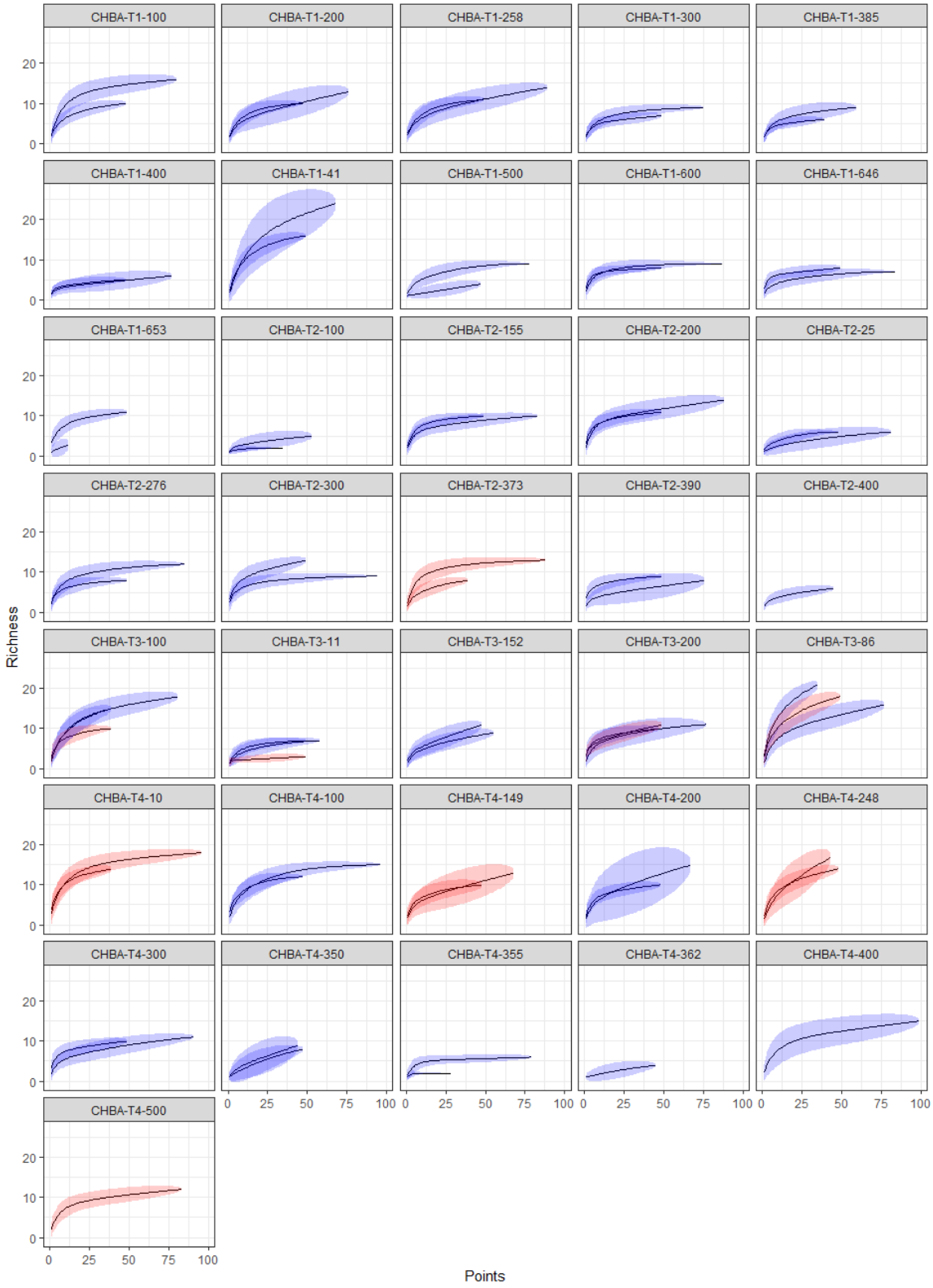

Figure A-4. Species accumulation curves and 1-SD envelopes for vegetation plots in Chinitna Bay. Color distinguishes plots oriented east from the transect (blue) from transects oriented west from the transect (red).

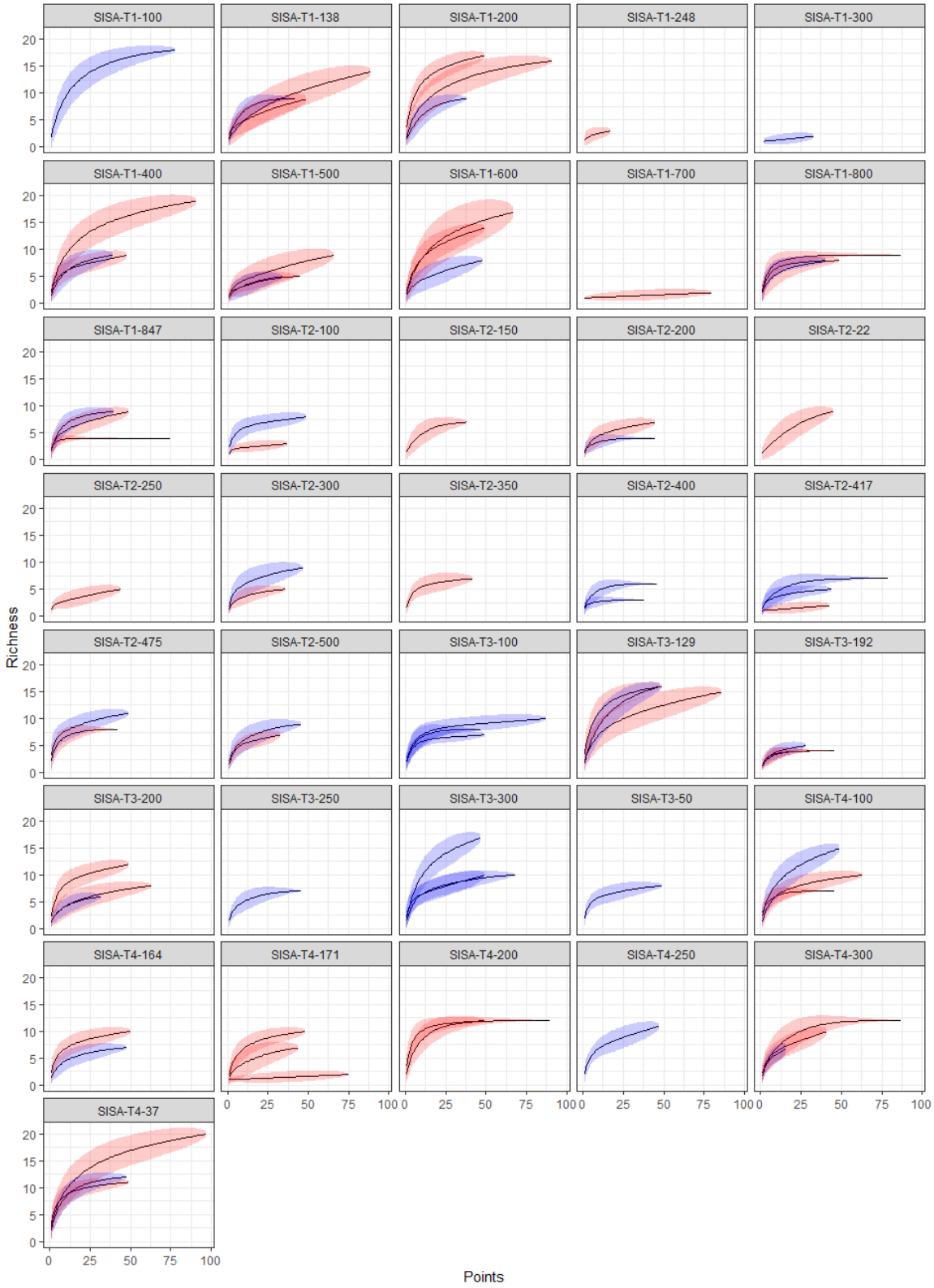

Figure A-5. Species accumulation curves and 1-SD envelopes for vegetation plots in Silver Salmon Creek. Color distinguishes plots oriented south from the transect (blue) from transects oriented north from the transect (red).

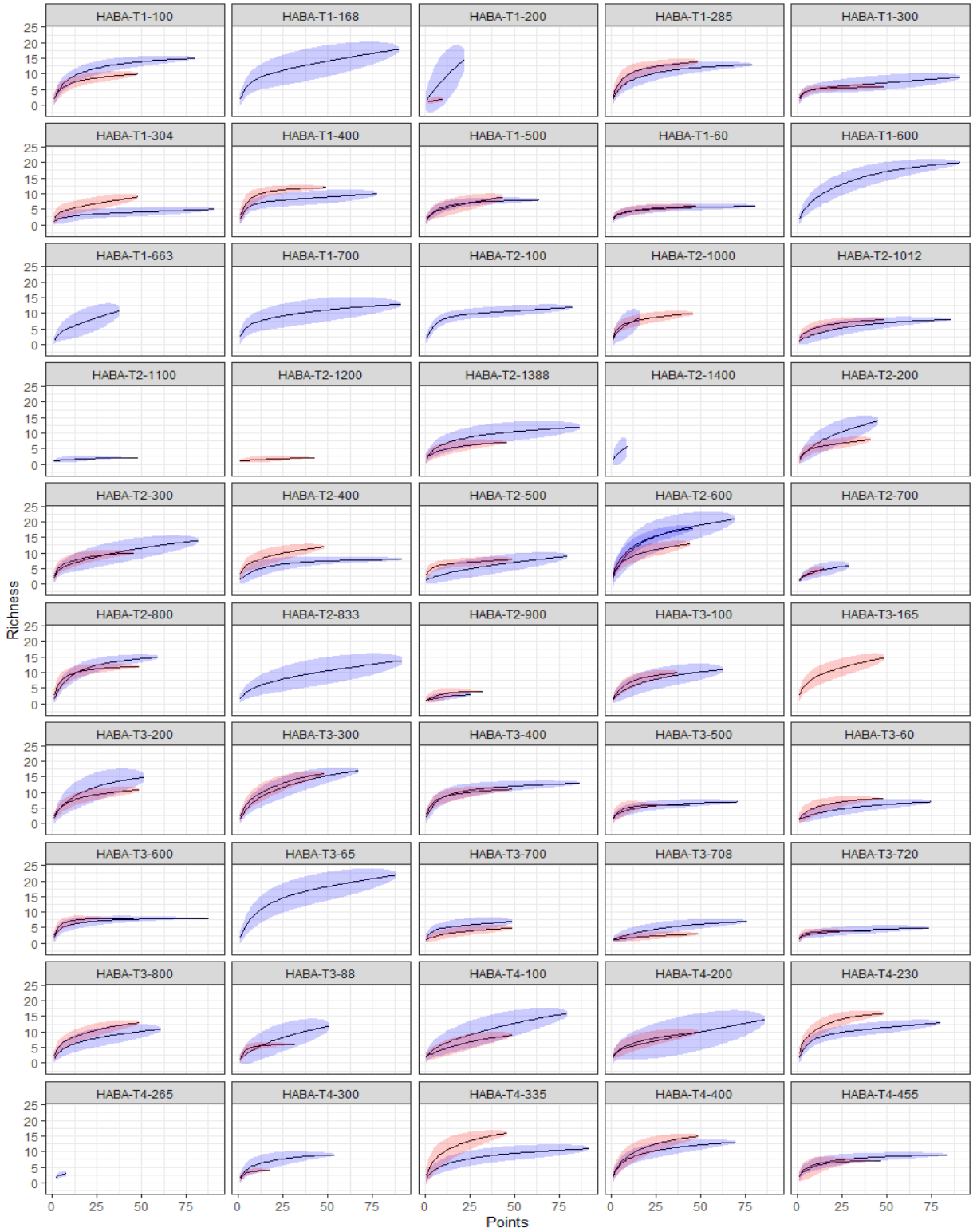

Figure A-6. Species accumulation curves and 1-SD envelopes for vegetation plots in Hallo Bay. Color distinguishes plots oriented south from the transect (blue) from transects oriented north from the transect (red).

Appendix B: Taxonomic Codes

Table B-1. Taxonomic codes and full scientific names reported by Jorgenson et al. (2010) and recorded in 2018 re-surveys. Currently accepted scientific names are listed as published in the Flora of North America (http://beta.floranorthamerica.org/Main_Page) and/or reported by the Consortium of Pacific Northwest Herbaria (http://www.pnwherbaria.org; accessed 27 April 2020). Where current accepted names are identical to those used by Jorgenson et al. (2010), the latter columns contain a dash (–). NR = taxon not reported in Jorgenson et al. (2010). NT = treatment not yet published in FNA.

Taxon Code	Jorgenson et al. (2010)	FNA – accepted	PNW – current accepted
ACHMIL	*Achillea millefolium L.*	–	–
AGRMER	*Agrostis mertensii Trin.*	–	–
AGRSCA	*Agrostis scabra Willd.*	–	–
ALNVIRS	*Alnus sinuata (Regel) Rydb.*	*Alnus viridis subsp. sinuata (Regel) Á. Löve & D. Löve*	*Alnus viridis subsp. sinuata (Regel) Á. Löve & D. Löve*
ANGGEN	*Angelica genuflexa Nutt.*	*NT*	*Angelica genuflexa Nutt.*
ANGLUC	*Angelica lucida L.*	*NT*	*Angelica lucida L.*
ATRGME	*Atriplex gmelinii C.A. Mey. ex Bong.*	–	–
BETDUG*	*NR*	*Betula × dugleana Lepage (= Betula glandulosa Michaux × B. neoalaskana Sargent)*	*Betula × dugleana Lepage (= Betula glandulosa Michaux × B. neoalaskana Sargent)*
BETKEN*	*Betula papyrifera var. kenaica (W. H. Evans) A. Henry*	*Betula kenaica W. H. Evans*	*Betula kenaica W. H. Evans*
BETNAN	*Betula nana L.*	–	–
BETNEO*	*NR*	*Betula neoalaskana Sarg.*	*Betula neoalaskana Sarg.*
BISVIV	*Polygonum viviparum L.*	*Bistorta vivipara (L.) Delarbre*	*Bistorta vivipara (L.) Delarbre*
CALCAN	*Calamagrostis canadensis (Michx.) P. Beauv.*	–	–
CALDES	*Calamagrostis deschampsioides Trin.*	–	–
CARAQU	*Carex aquatilis Wahlenb. var. aquatilis*	*Carex aquatilis Wahlenb. var. aquatilis*	*Carex aquatilis Wahlenb.*
CARCANC	*Carex canescens L.*	*Carex canescens L.*	*Carex canescens L. subsp. canescens*
CARDA	*Cardamine L.*	–	–

* Jorgenson et al. (2010) reported Betula papyrifera var. kenaica, which was recorded alternatively as Betula × dugleana and Betula neoalaskana in 2018. For the purposes of this report, we assume that all records for these two taxa refer to B. papyrifera var. kenaica (= B. kenaica).

** Jorgenson et al. (2010) reported Potamogeton filiformis, which was recorded as Potamogeton sp., Stuckenia filiformis, and Stuckenia pectinata in 2018.

Table B-1 (continued). Taxonomic codes and full scientific names reported by Jorgenson et al. (2010) and recorded in 2018 re-surveys. Currently accepted scientific names are listed as published in the Flora of North America (http://beta.floranorthamerica.org/Main_Page) and/or reported by the Consortium of Pacific Northwest Herbaria (http://www.pnwherbaria.org; accessed 27 April 2020). Where current accepted names are identical to those used by Jorgenson et al. (2010), the latter columns contain a dash (–). NR = taxon not reported in Jorgenson et al. (2010). NT = treatment not yet published in FNA.

Taxon Code	Jorgenson et al. (2010)	FNA – accepted	PNW – current accepted
CAREX	*Carex L.*	–	–
CARGLAG	*Carex glareosa Wahlenb.*	*Carex glareosa Wahlenb.*	*Carex glareosa Wahlenb. subsp. glareosa*
CARGME	*Carex gmelinii Hook. & Arn.*	–	–
CARLYN	*Carex lyngbyei Hornem.*	–	–
CARMAC	*Carex mackenziei V.I. Krecz.*	–	–
CARMAC2	*Carex macrocephala Willd. ex Spreng.*	–	–
CARMAC3	*Carex macrochaeta C.A. Mey.*	–	–
CARPLU	*Carex pluriflora Hultén*	–	–
CARRAM	*Carex ramenskii Kom.*	–	–
CARUTR	*Carex utriculata Boott*	–	–
CHAANG	*Epilobium angustifolium L.*	*NT*	*Chamaenerion angustifolium (L.) Scop.*
CHRARC	*Chrysanthemum arcticum L.*	*Arctanthemum arcticum (L.) Tzvelev*	*Arctanthemum arcticum (L.) Tzvelev*
CICVIR	*Cicuta virosa L.*	–	–
COMPAL	*Potentilla palustris (L.) Scop.*	*Comarum palustre L.*	*Comarum palustre L.*
CONCHI	*Conioselinum chinense (L.) Britton, Sterns & Poggenb.*	*NT*	*Conioselinum chinense (L.) Britton, Sterns & Poggenb.*
CORSUE	*Cornus suecica L.*	–	–
DESCESB	*Deschampsia beringensis Hultén*	*Deschampsia cespitosa (L.) P. Beauv. subsp. beringensis (Hulten) W.E. Lawr.*	*Deschampsia cespitosa (L.) P. Beauv.*
DRYEXP	*Dryopteris dilatata (Hoffm.) A. Gray subsp. americana (Fisch.) Hultén*	*Dryopteris expansa (C. Presl) Fraser-Jenk. & Jermy*	*Dryopteris expansa (C. Presl) Fraser-Jenk. & Jermy*
ELEPAL	*Eleocharis palustris (L.) Roem. & Schult.*	–	–

* Jorgenson et al. (2010) reported Betula papyrifera var. kenaica, which was recorded alternatively as Betula × dugleana and Betula neoalaskana in 2018. For the purposes of this report, we assume that all records for these two taxa refer to B. papyrifera var. kenaica (= B. kenaica).

** Jorgenson et al. (2010) reported Potamogeton filiformis, which was recorded as Potamogeton sp., Stuckenia filiformis, and Stuckenia pectinata in 2018.

Table B-1 (continued). Taxonomic codes and full scientific names reported by Jorgenson et al. (2010) and recorded in 2018 re-surveys. Currently accepted scientific names are listed as published in the Flora of North America (http://beta.floranorthamerica.org/Main_Page) and/or reported by the Consortium of Pacific Northwest Herbaria (http://www.pnwherbaria.org; accessed 27 April 2020). Where current accepted names are identical to those used by Jorgenson et al. (2010), the latter columns contain a dash (–). NR = taxon not reported in Jorgenson et al. (2010). NT = treatment not yet published in FNA.

Taxon Code	Jorgenson et al. (2010)	FNA – accepted	PNW – current accepted
EPIPAL	*Epilobium palustre L.*	*NT*	*Epilobium palustre L.*
EQUARV	*Equisetum arvense L.*	–	–
EQUFLU	*Equisetum fluviatile L.*	–	–
ERIRUS	*Eriophorum russeolum Fr.*	–	–
FESRUB	*Festuca rubra L.*	–	–
FRICAM	*Fritillaria camschatcensis (L.) Ker Gawl.*	–	–
GALAPA	*NR*	*NT*	*Galium aparine L.*
GALTRI	*Galium trifidum L. subsp. trifidum*	*NT*	*Galium trifidum L.*
GERERI	*Geranium erianthum DC.*	–	–
GRASS	*NR – Unknown grass*	–	–
HERMAX	*NR*	*NT*	*Heracleum maximum Bartr.*
HIEODO	*Hierochloe odorata (L.) P. Beauv.*	–	–
HIPTET	*Hippuris tetraphylla L. f.*	–	–
HIPVUL	*Hippuris vulgaris L.*	–	–
HONPEP	*Honckenya peploides (L.) Ehrh.*	–	–
HORBRA	*Hordeum brachyantherum Nevski*	–	–
IRISET	*Iris setosa Pall. ex Link*	–	–
JUNARC	*Juncus arcticus Willd.*	–	–
LATJAP	*NR*	*NT*	*Lathyrus japonicus Willd.*
LATMAR	*Lathyrus maritimus (L.) Bigelow subsp. maritimus*	*NT*	*Lathyrus maritimus (L.) Bigelow subsp. maritimus*
LATPAL	*Lathyrus palustris L.*	*NT*	*Lathyrus palustris L.*
LEYMOLM	*Elymus arenarius L. subsp. mollis (Trin.) Hultén*	*Leymus mollis (Trin.) Pilg.*	*Leymus mollis (Trin.) Pilg. subsp. mollis*

* Jorgenson et al. (2010) reported Betula papyrifera var. kenaica, which was recorded alternatively as Betula × dugleana and Betula neoalaskana in 2018. For the purposes of this report, we assume that all records for these two taxa refer to B. papyrifera var. kenaica (= B. kenaica).

** Jorgenson et al. (2010) reported Potamogeton filiformis, which was recorded as Potamogeton sp., Stuckenia filiformis, and Stuckenia pectinata in 2018.

Table B-1 (continued). Taxonomic codes and full scientific names reported by Jorgenson et al. (2010) and recorded in 2018 re-surveys. Currently accepted scientific names are listed as published in the Flora of North America (http://beta.floranorthamerica.org/Main_Page) and/or reported by the Consortium of Pacific Northwest Herbaria (http://www.pnwherbaria.org; accessed 27 April 2020). Where current accepted names are identical to those used by Jorgenson et al. (2010), the latter columns contain a dash (–). NR = taxon not reported in Jorgenson et al. (2010). NT = treatment not yet published in FNA.

Taxon Code	Jorgenson et al. (2010)	FNA – accepted	PNW – current accepted
LIGSCO	*Ligusticum scoticum L.*	*NT*	*Ligusticum scoticum L. subsp. hultenii (Fernald) Calder & Roy L. Taylor*
LUPNOO	*Lupinus nootkatensis Donn ex Sims*	*NT*	*Lupinus nootkatensis Donn ex Sims*
TRIEUR	*Trientalis europaea L.*	*Trientalis europaea L.*	*Lysimachia europaea (L.) U. Manns & Anderb.*
LYSMAR	*NR*	*Lysimachia maritima (L.) Galasso*	*Lysimachia maritima (L.) Galasso, Banfi & Soldano*
MERMARM	*Mertensia maritima (L.) Gray*	*NT*	*Mertensia maritima (L.) Gray var. maritima*
MOELAT	*Moehringia lateriflora (L.) Fenzl*	–	–
MYRGAL	*Myrica gale L.*	–	–
MYRIO	*Myriophyllum L.*	*NT*	*Myriophyllum L.*
PARPAL	*NR*	*Parnassia palustris L.*	*Parnassia palustris L.*
PHLALP	*Phleum alpinum L.*	–	–
PICSIT	*Picea sitchensis (Bong.) Carrière*	–	–
PLAMAR	*Plantago maritima L.*	–	–
POA	*Poa L.*	–	–
POAARC	*Poa arctica R. Br.*	–	–
POAEMI	*Poa eminens J. Presl*	*Poa eminens J. Presl*	*Arctopoa eminens (J. Presl) Prob.*
POAMAC	*NR*	*Poa macrocalyx Trautv. & C.A. Mey.*	*Poa macrocalyx Trautv. & C.A. Mey.*
POLACU	*Polemonium acutiflorum Willd.*	*NT*	*Polemonium caeruleum L. subsp. villosum (J.H. Rudolph ex Georgi) Brand*
POTAM**	*NR*	*Potamogeton L.*	*Potamogeton L.*
POTANSP	*Potentilla egedii Wormsk.*	*Potentilla anserina L. subsp. pacifica (Howell) Rousi*	*Potentilla anserina L. subsp. pacifica (Howell) Rousi*

* Jorgenson et al. (2010) reported Betula papyrifera var. kenaica, which was recorded alternatively as Betula × dugleana and Betula neoalaskana in 2018. For the purposes of this report, we assume that all records for these two taxa refer to B. papyrifera var. kenaica (= B. kenaica).

** Jorgenson et al. (2010) reported Potamogeton filiformis, which was recorded as Potamogeton sp., Stuckenia filiformis, and Stuckenia pectinata in 2018.

Table B-1 (continued). Taxonomic codes and full scientific names reported by Jorgenson et al. (2010) and recorded in 2018 re-surveys. Currently accepted scientific names are listed as published in the Flora of North America (http://beta.floranorthamerica.org/Main_Page) and/or reported by the Consortium of Pacific Northwest Herbaria (http://www.pnwherbaria.org; accessed 27 April 2020). Where current accepted names are identical to those used by Jorgenson et al. (2010), the latter columns contain a dash (–). NR = taxon not reported in Jorgenson et al. (2010). NT = treatment not yet published in FNA.

Taxon Code	Jorgenson et al. (2010)	FNA – accepted	PNW – current accepted
PUCGRA	*Puccinellia grandis Swallen*	*Puccinellia nutkaensis (J. Presl) Fern. & Weath.*	*Puccinellia nutkaensis (J. Presl) Fern. & Weath.*
PUCPHR	*Puccinellia phryganodes (Trin.) Scribn. & Merr.*	–	–
RHIMING	*Rhinanthus minor L. subsp. borealis (Sterneck) Á. Löve*	*Rhinanthus minor L. subsp. groenlandicus (Chabert) Neum.*	*Rhinanthus minor L. subsp. groenlandicus (Chabert) Neum.*
RHOMEN	*NR*	*Menziesia ferruginea Smith*	*Rhododendron menziesii Craven*
RUBARC	*Rubus arcticus L.*	–	–
RUMOCC	*Rumex fenestratus Greene*	*Rumex occidentalis S. Watson*	*Rumex occidentalis S. Watson*
SALBAR	*Salix barclayi Andersson*	–	–
SALFUS	*Salix fuscescens Andersson*	–	–
SALPUL	*Salix planifolia Pursh subsp. pulchra (Cham.) Argus*	*Salix pulchra Cham.*	*Salix pulchra Cham.*
SANSTI	*NR*	*Sanguisorba stipulata Raf.*	*Sanguisorba stipulata Raf.*
SAUNUD	*Saussurea nuda Ledeb.*	–	–
SENPSE	*Senecio pseudoarnica Less.*	–	–
SPAANG	*Sparganium angustifolium Michx.*	–	–
STECAL	*Stellaria calycantha (Ledeb.) Bong.*	–	–
STECRA	*Stellaria crassifolia Ehrh.*	–	–
STECRI	*Stellaria crispa Cham. & Schltdl.*	–	–
STEHUM	*Stellaria humifusa Rottb.*	–	–
STELL	*Stellaria L.*	–	–
STUFIL**	*Potamogeton filiformis Pers.*	*Stuckenia filiformis (Pers.) Börner*	*Stuckenia filiformis (Pers.) Börner*

* Jorgenson et al. (2010) reported Betula papyrifera var. kenaica, which was recorded alternatively as Betula × dugleana and Betula neoalaskana in 2018. For the purposes of this report, we assume that all records for these two taxa refer to B. papyrifera var. kenaica (= B. kenaica).

** Jorgenson et al. (2010) reported Potamogeton filiformis, which was recorded as Potamogeton sp., Stuckenia filiformis, and Stuckenia pectinata in 2018.

Table B-1 (continued). Taxonomic codes and full scientific names reported by Jorgenson et al. (2010) and recorded in 2018 re-surveys. Currently accepted scientific names are listed as published in the Flora of North America (http://beta.floranorthamerica.org/Main_Page) and/or reported by the Consortium of Pacific Northwest Herbaria (http://www.pnwherbaria.org; accessed 27 April 2020). Where current accepted names are identical to those used by Jorgenson et al. (2010), the latter columns contain a dash (–). NR = taxon not reported in Jorgenson et al. (2010). NT = treatment not yet published in FNA.

Taxon Code	Jorgenson et al. (2010)	FNA – accepted	PNW – current accepted
STUPEC**	*Potamogeton pectinatus L.*	*Stuckenia pectinata (L.) Borner*	*Stuckenia pectinata (L.) Borner*
TRIMAR	*Triglochin maritima L.*	–	–
TRIPAL	*Triglochin palustris L.*	–	–
VIOLA	*Viola L.*	–	–
VIOLAN	*Viola langsdorffii Fisch. ex Ging.*	–	–

* Jorgenson et al. (2010) reported *Betula papyrifera* var. *kenaica*, which was recorded alternatively as *Betula* × *dugleana* and *Betula neoalaskana* in 2018. For the purposes of this report, we assume that all records for these two taxa refer to *B. papyrifera* var. *kenaica* (= *B. kenaica*).

** Jorgenson et al. (2010) reported *Potamogeton filiformis*, which was recorded as *Potamogeton* sp., *Stuckenia filiformis*, and *Stuckenia pectinata* in 2018.

Appendix C: Generalized Linear Mixed Model Description

To assess changes in the cover for individual species we developed a generalized linear mixed effects model (GLMM) of point-intercept data. The number of hits for a species at plot i and year t, ($y_{i,t}$) was modeled with a binomial error distribution, as a function of the probability of a hit ($P_{i,t}$), equivalent to cover within the plot, and the number of intercept points ($N_{i,t}$).

$$y_{i,t} \sim \text{binomial}(P_{i,t}, N_{i,t})$$

The logit of cover ($P_{i,t}$) was, in turn, modeled as a linear function of grouping variables and year.

$$log\left(\frac{P_{i,t}}{1-P_{i,t}}\right) = \alpha_i + \beta_i \cdot year_t$$

Where α_i, and β_i are plot-level random intercepts and slopes, respectively. These plot-level random effects were nested in plot-blocks. Let $b[i]$ index the block that plot i belongs to, then $\gamma_{b[i]}$, and $\phi_{b[i]}$ are the block-level random intercepts and slopes for plot i.

$$\alpha_i \sim \mathcal{N}\left(\gamma_{b[i]}, \varsigma^{\alpha}\right)$$

$$\beta_i \sim \mathcal{N}\left(\delta_{b[i]}, \varsigma^{\beta}\right)$$

$$\gamma_{b[i]} \sim \mathcal{N}(\mu, \sigma)$$

$$\delta_{b[i]} \sim \mathcal{N}(\zeta, \eta)$$

We made inference from this model in a Bayesian framework. Bayes' theorem allows that the posterior probability of our model parameters, given our data, is proportional to the joint distribution of the likelihood and prior probabilities. For our model:

$$\left[\alpha_i, \beta_i, \gamma_{b[i]}, \delta_{b[i]}, \varsigma^{\alpha}, \varsigma^{\beta}, \nu, \sigma, \eta \mid y_{i,t}\right]$$

$$\propto \prod_{t=1}^{T}\prod_{i=1}^{N} Binomial\left[y_{i,t} \mid n_i, g(\alpha_i, \beta_i, year_i, H_i)\right] \times \mathcal{N}[\alpha_i \mid \gamma_{b[i]}, \sigma^2] \times \mathcal{N}[\beta_i \mid \delta_{b[i]}, \varsigma^{\beta}] \times \mathcal{N}[\gamma_{b[i]} \mid \mu, \varsigma^{\alpha}] \times \mathcal{N}[\delta_{b[i]} \mid \zeta, \varsigma^{\alpha}] \times t_1[\mu \mid 0{,}10] \times t_1[\zeta \mid 0{,}2.5] \times |\mathcal{N}[\varsigma^{\alpha} \mid 0{,}25]| \times \left|\mathcal{N}\left[\varsigma^{\beta} \mid 0{,}25\right]\right| \times |\mathcal{N}[\sigma \mid 0{,}25]| \times |\mathcal{N}[\eta \mid 0{,}25]|$$

Where:

$$g(\alpha_i, \beta_i, year_i, H_i) = \text{logit}^{-1}(\alpha_i + \beta_i \cdot year_t) \cdot H_i$$

We used vague prior probabilities. We used Students t distribution with one degree of freedom and a scale parameter of 10 or 2.5 for priors on model intercepts and slopes, respectively, as recommended by Gelman et al. (2008). For random effect variances, we used a folded normal distribution with mean of 0 and standard deviation of 25 (Gelman 2006). All predictor variables were centered and scaled by subtracting their mean and dividing by two standard deviations (Gelman 2008).

To assess changes in the cover for functional groups we used a similar generalized linear mixed effects model (GLMM) of point-intercept data. Because the total cover of multiple species can exceed the number of sample points, the number of hits for a functional group at plot i and year t, ($y_{i,t}$) was modeled with a Poisson error distribution, as a function of the rate parameter ($\lambda_{i,t}$), equivalent to mean number of hits within the plot.

$$y_{i,t} \sim \text{Poisson}(\lambda_{i,t})$$

The rate was, in turn, modeled as a linear function of grouping variables and year, and an offset of the number of intercept points ($N_{i,t}$), using an exponential link function.

$$\lambda_{i,t} = e^{\alpha_i + \beta_i \cdot year_t + N_{i,t}}$$

Where α_i, and β_i are plot-level random intercepts and slopes, respectively. These plot-level random effects were nested in plot-blocks. Let $b[i]$ index the block that plot i belongs to, then $\gamma_{b[i]}$, and $\phi_{b[i]}$ are the block-level random intercepts and slopes for plot i.

$$\alpha_i \sim \mathcal{N}(\gamma_{b[i]}, \varsigma^{\alpha})$$

$$\beta_i \sim \mathcal{N}(\delta_{b[i]}, \varsigma^{\beta})$$

$$\gamma_{b[i]} \sim \mathcal{N}(\mu, \sigma)$$

$$\delta_{b[i]} \sim \mathcal{N}(\zeta, \eta)$$

We made inference from this model in a Bayesian framework. Bayes' theorem allows that the posterior probability of our model parameters, given our data, is proportional to the joint distribution of the likelihood and prior probabilities. For our model:

$$\left[\alpha_i, \beta_i, \gamma_{b[i]}, \delta_{b[i]}, \varsigma^{\alpha}, \varsigma^{\beta}, \nu, \sigma, \eta \mid y_{i,t}\right]$$

$$\propto \prod_{t=1}^{T} \prod_{i=1}^{N} Poisson\left[y_{i,t} \mid g(\alpha_i, \beta_i, year_i, N_{i,t})\right] \times \mathcal{N}\left[\alpha_i \mid \gamma_{b[i]}, \sigma^2\right] \times \mathcal{N}\left[\beta_i \mid \delta_{b[i]}, \varsigma^{\beta}\right] \times \mathcal{N}\left[\gamma_{b[i]} \mid \mu, \varsigma^{\alpha}\right] \times \mathcal{N}\left[\delta_{b[i]} \mid \zeta, \varsigma^{\alpha}\right] \times \mathcal{N}\left[\mu \mid 0{,}1000\right] \times \mathcal{N}\left[\zeta \mid 0{,}1000\right] \times \left|\mathcal{N}\left[\varsigma^{\alpha} \mid 0{,}25\right]\right| \times \left|\mathcal{N}\left[\varsigma^{\beta} \mid 0{,}25\right]\right| \times \left|\mathcal{N}\left[\sigma \mid 0{,}25\right]\right| \times \left|\mathcal{N}\left[\eta \mid 0{,}25\right]\right|$$

Where:

$$g\left(\alpha_i, \beta_i, year_t, N_{i,t}\right) = e^{\alpha_i + \beta_i \cdot year_t + N_{i,t}}$$

We used vague prior probabilities. We used Gaussian with mean 0 and a variance of 1000 for priors on model intercepts and slopes. For random effect variances, we used a folded normal distribution with mean of 0 and standard deviation of 25 (Gelman 2006). All predictor variables were centered and scaled by subtracting their mean and dividing by two standard deviations (Gelman 2008).

We constructed and fit our model using JAGS (Plummer 2017) and the jagsUI package (Kellner 2018) in R (R Core Team 2019). We sampled the posterior distribution of the model parameters given out data using Markov Chain Monte Carlo (MCMC). Each of three MCMC chain was burned in for at least 5000 iterations or until all chains converged according to the Gelman-Rubin statistic (Gelman & Rubin 1992) and visual scrutiny. To test model adequacy, we calculated Bayesian P-values (Conn et al. 2018), for the mean and standard deviation of number of hits at each plot. We present parameter estimates and model predictions as the posterior mean $\pm$ 95% credible intervals.

Appendix D: Supplemental Tables

Table D-1. Species cover and frequency recorded in 2018, by site, for sites in LACL and KATM. CHBA = Chinitna Bay; HABA = Hallo Bay; SISA = Silver Salmon Creek. Cover was estimated by point intercept. Frequency indicates the proportion of plots in which a species was found. Unless otherwise noted, nomenclature follows Jorgenson et al. (2010).

	Mean Cover			Max Cover			Frequency		
Species Name	**CHBA**	**HABA**	**SISA**	**CHBA**	**HABA**	**SISA**	**CHBA**	**HABA**	**SISA**
Festuca rubra	0.26	0.12	0.23	0.92	0.68	0.98	0.73	0.54	0.54
Lathyrus japonicus	0.21	0.06	0.06	0.86	0.84	0.34	0.49	0.29	0.36
Elymus mollis subsp. *mollis*	0.21	0.23	0.12	0.96	1.00	0.80	0.43	0.49	0.56
Carex lyngbyei	0.19	0.16	0.15	1.00	1.00	1.00	0.43	0.39	0.26
Calamagrostis canadensis	0.14	0.18	0.05	0.74	0.96	0.86	0.43	0.49	0.20
Achillea millefolium	0.11	0.13	0.17	0.68	0.92	0.82	0.41	0.32	0.43
Carex pluriflora	0.11	0.02	0.00	0.94	0.58	0.14	0.27	0.05	0.03
Carex glareosa subsp. *glareosa*	0.09	0.04	0.07	0.96	0.62	0.60	0.24	0.12	0.33
Carex gmelinii	0.07	0.03	0.04	0.60	0.38	0.38	0.35	0.17	0.26
Salix fuscescens	0.06	0.04	0.01	0.60	0.54	0.30	0.16	0.17	0.07
Triglochin maritima	0.06	0.03	0.14	0.64	0.34	0.88	0.30	0.34	0.44
Hordeum brachyantherum	0.06	0.00	0.03	0.54	0.00	0.62	0.22	0.00	0.13
Picea sitchensis	0.05	0.00	0.05	0.44	0.00	0.90	0.24	0.00	0.18
Equisetum fluviatile	0.05	0.00	0.00	0.66	0.00	0.00	0.11	0.00	0.00
Myrica gale	0.04	0.10	0.00	0.58	0.76	0.00	0.16	0.22	0.00
Poa eminens	0.04	0.05	0.03	0.40	0.64	0.56	0.27	0.24	0.25
Potentilla egedii	0.04	0.07	0.04	0.32	0.64	0.36	0.27	0.29	0.36
Angelica lucida	0.04	0.02	0.03	0.34	0.18	0.38	0.38	0.22	0.30
Poa macrocalyx	0.04	0.00	0.00	0.46	0.00	0.00	0.30	0.00	0.00
Potentilla palustre	0.03	0.02	0.00	0.44	0.56	0.04	0.30	0.17	0.05
Cicuta virosa	0.02	0.00	0.00	0.56	0.04	0.00	0.14	0.12	0.00

Species Name	Mean Cover			Max Cover			Frequency		
	CHBA	HABA	SISA	CHBA	HABA	SISA	CHBA	HABA	SISA
Equisetum arvense	0.02	0.00	0.00	0.50	0.00	0.00	0.14	0.00	0.00
Potamogeton filiformis	0.02	0.00	0.00	0.72	0.10	0.04	0.03	0.02	0.02
Salix barclayi	0.02	0.02	0.00	0.54	0.40	0.00	0.03	0.07	0.00
Chrysanthemum arcticum	0.01	0.01	0.01	0.12	0.20	0.16	0.24	0.22	0.18
Triglochin palustris	0.01	0.01	0.01	0.26	0.16	0.16	0.14	0.15	0.18
Carex ramenskii	0.01	0.12	0.04	0.48	0.90	0.60	0.03	0.34	0.15
Ligusticum scoticum subsp. *hultenii*	0.01	0.02	0.00	0.20	0.44	0.12	0.14	0.24	0.03
Moehringia lateriflora	0.01	0.01	0.03	0.08	0.08	0.38	0.27	0.29	0.30
Hierochloe odorata	0.01	0.00	0.00	0.38	0.00	0.02	0.03	0.00	0.02
Galium trifidum subsp. *trifidum*	0.01	0.01	0.01	0.06	0.06	0.22	0.22	0.17	0.15
Hippuris tetraphylla	0.01	0.00	0.00	0.24	0.00	0.10	0.05	0.00	0.03
Honckenya peploides	0.01	0.00	0.00	0.18	0.00	0.04	0.08	0.00	0.02
Agrostis scabra	0.01	0.00	0.00	0.10	0.00	0.20	0.08	0.00	0.02
Lathyrus palustris	0.01	0.03	0.00	0.18	0.58	0.06	0.08	0.17	0.02
Rhinanthus minor subsp. *groenlandicus*	0.01	0.00	0.01	0.12	0.06	0.18	0.16	0.10	0.20
Carex aquatilis	0.01	0.00	0.00	0.16	0.02	0.10	0.05	0.02	0.02
Conioselinum chinense	0.00	0.01	0.01	0.06	0.10	0.26	0.14	0.27	0.18
Polemonium acutiflorum	0.00	0.00	0.00	0.10	0.00	0.00	0.08	0.00	0.00
Sanguisorba stipulata	0.00	0.00	0.00	0.08	0.00	0.00	0.11	0.00	0.00
Betula nana	0.00	0.00	0.00	0.10	0.00	0.00	0.03	0.00	0.00
Juncus arcticus	0.00	0.00	0.00	0.10	0.02	0.10	0.05	0.02	0.03
Senecio pseudoarnica	0.00	0.00	0.00	0.12	0.06	0.00	0.03	0.05	0.00
Trientalis europaea	0.00	0.01	0.01	0.02	0.18	0.08	0.16	0.22	0.23
Betula neoalaskana	0.00	0.01	0.00	0.06	0.42	0.00	0.05	0.07	0.00
Carex sp.	0.00	0.00	0.00	0.04	0.00	0.10	0.08	0.00	0.07

Species Name	Mean Cover			Max Cover			Frequency		
	CHBA	HABA	SISA	CHBA	HABA	SISA	CHBA	HABA	SISA
Dryopteris expansa	0.00	0.00	0.00	0.08	0.00	0.00	0.03	0.00	0.00
Epilobium palustre	0.00	0.00	0.00	0.06	0.00	0.00	0.05	0.00	0.00
Puccinellia phryganodes	0.00	0.02	0.02	0.04	0.32	0.40	0.05	0.17	0.07
Rumex occidentalis S. Watson	0.00	0.00	0.00	0.06	0.00	0.00	0.03	0.00	0.00
Salix pulchra	0.00	0.00	0.00	0.04	0.08	0.00	0.05	0.02	0.00
Viola sp.	0.00	0.00	0.00	0.08	0.00	0.00	0.03	0.00	0.00
Angelica genuflexa	0.00	0.00	0.00	0.02	0.00	0.00	0.03	0.00	0.00
Betula × dugleana	0.00	0.00	0.00	0.02	0.00	0.00	0.03	0.00	0.00
Deschampsia beringensis	0.00	0.00	0.00	0.04	0.00	0.00	0.03	0.00	0.00
Lupinus nootkatensis	0.00	0.02	0.02	0.04	0.30	0.36	0.03	0.20	0.15
Parnassia palustris	0.00	0.00	0.00	0.02	0.00	0.00	0.03	0.00	0.00
Polygonum vivipara	0.00	0.00	0.00	0.02	0.00	0.00	0.03	0.00	0.00
Poa sp.	0.00	0.00	0.00	0.02	0.02	0.04	0.03	0.02	0.03
Stellaria humifusa	0.00	0.03	0.00	0.02	0.36	0.18	0.03	0.15	0.05
Stellaria sp.	0.00	0.00	0.00	0.02	0.00	0.00	0.03	0.00	0.00
Plantago maritima	0.00	0.08	0.07	0.00	0.76	1.00	0.00	0.22	0.16
Epilobium angustifolium	0.00	0.05	0.01	0.00	0.68	0.24	0.00	0.22	0.07
Deschampsia beringensis	0.00	0.04	0.00	0.00	0.84	0.00	0.00	0.22	0.00
Iris setosa	0.00	0.03	0.01	0.00	0.28	0.18	0.00	0.17	0.05
Geranium erianthum	0.00	0.02	0.00	0.00	0.16	0.06	0.00	0.12	0.02
Rubus arcticus	0.00	0.01	0.01	0.00	0.18	0.18	0.00	0.15	0.08
Eleocharis kamtschatica	0.00	0.01	0.00	0.00	0.18	0.00	0.00	0.10	0.00
Carex macrochaeta	0.00	0.01	0.00	0.00	0.32	0.00	0.00	0.02	0.00
Carex mackenziei	0.00	0.01	0.03	0.00	0.14	0.48	0.00	0.05	0.12
Puccinellia nutkaensis	0.00	0.01	0.01	0.00	0.12	0.52	0.00	0.05	0.07
Calamagrostis deschampsioides	0.00	0.01	0.01	0.00	0.16	0.38	0.00	0.07	0.07

Species Name	Mean Cover			Max Cover			Frequency		
	CHBA	HABA	SISA	CHBA	HABA	SISA	CHBA	HABA	SISA
Cornus suecica	0.00	0.00	0.00	0.00	0.08	0.00	0.00	0.02	0.00
Drosera rotundifolia	0.00	0.00	0.00	0.00	0.08	0.00	0.00	0.02	0.00
Stellaria crassifolia	0.00	0.00	0.00	0.00	0.10	0.08	0.00	0.02	0.05
Alnus sinuata	0.00	0.00	0.00	0.00	0.04	0.00	0.00	0.02	0.00
Fritillaria camschatcensis	0.00	0.00	0.01	0.00	0.04	0.08	0.00	0.02	0.13
Mertensia maritima var. *maritima*	0.00	0.00	0.00	0.00	0.02	0.00	0.00	0.02	0.00
Potamogeton sp.	0.00	0.00	0.00	0.00	0.02	0.00	0.00	0.02	0.00
Puccinellia grandis	0.00	0.00	0.00	0.00	0.02	0.00	0.00	0.02	0.00
Poa arctica	0.00	0.00	0.05	0.00	0.00	0.60	0.00	0.00	0.20
Eleocharis palustris	0.00	0.00	0.03	0.00	0.00	0.86	0.00	0.00	0.08
Agrostis mertensii	0.00	0.00	0.01	0.00	0.00	0.24	0.00	0.00	0.07
Carex macrocephala	0.00	0.00	0.01	0.00	0.00	0.40	0.00	0.00	0.03
Geum macrophyllum var. *macrophyllum*	0.00	0.00	0.00	0.00	0.00	0.04	0.00	0.00	0.02
Phleum alpinum	0.00	0.00	0.00	0.00	0.00	0.02	0.00	0.00	0.02
Rubus arcticus subsp. *stellatus*	0.00	0.00	0.00	0.00	0.00	0.02	0.00	0.00	0.02
Sparganium angustifolium	0.00	0.00	0.00	0.00	0.00	0.02	0.00	0.00	0.02

Table D-2. PERMANOVA of species proportional composition (species hits/total hits) for sites sampled in both intervals. P-values reflect significance in a test for no difference in species composition among levels of the identified factor. PERMANOVA is sensitive to differences in both the multivariate centroid and dispersion. A dash (–) indicates no data.

Model term	df	SS	MS	F	R^2	p
Geomorphic Group	**1.00**	**3.64**	**3.64**	**44.52**	**0.19**	**0.001**
Floristic Class	12.00	9.56	0.80	9.76	0.49	0.001
Plot ID	14.00	3.21	0.23	2.81	0.16	0.999
Occasion	1.00	0.41	0.41	5.00	0.02	0.001
Geomorphic Group × Occasion	1.00	0.15	0.15	1.84	0.01	0.030
Floristic Class × Occasion	12.00	1.37	0.11	1.40	0.07	0.031
Residuals	14.00	1.14	0.08	–	0.06	–
Total	55.00	19.48	–	–	1.00	–

Table D-3. PERMANOVA of species cover (species hits/plot points) for tidal flat sites sampled in both intervals. P-values reflect significance in a test for no difference in species composition among levels of the identified factor. PERMANOVA is sensitive to differences in both the multivariate centroid and dispersion. A dash (–) indicates no data.

Model Term	df	SS	MS	F	R2	p
Floristic_Class	**8.00**	**7.68**	**0.96**	**8.34**	**0.60**	**0.001**
Plot ID	9.00	2.34	0.26	2.26	0.18	0.842
Sample Event	1.00	0.56	0.56	4.89	0.04	0.001
Floristic Class x Sample Event	8.00	1.20	0.15	1.31	0.09	0.060
Residuals	9.00	1.04	0.12	–	0.08	–
Total	35.00	12.83	–	–	–	–

The Department of the Interior protects and manages the nation's natural resources and cultural heritage; provides scientific and other information about those resources; and honors its special responsibilities to American Indians, Alaska Natives, and affiliated Island Communities.

NPS 953/173876, December 2020

Natural Resource Stewardship and Science
1201 Oakridge Drive, Suite 150
Fort Collins, CO 80525